Therapeutic gene editing in hematopoietic progenitor cells from a mouse model of Fanconi anemia

Short title: Genome Editing in HSPCs from FA-A mice

Pino-Barrio MJ[1,2], Gimenez Y[1,2], Villanueva M[1,2], Hildenbeutel M[6,7], Sánchez-Dominguez R[1,2], Rodriguez-Perales S[3], Pujol R[4,5], Surrallés J[4,5], Rio P[1,2], Cathomen T[6,7,8], Mussolino C[6,7], Bueren JA[1,2*], Navarro S[1,2*].

[1]Division of Hematopoietic Innovative Therapies, CIEMAT/CIBERER, 28040 Madrid, Spain.

[2]Advanced Therapies Unit, IIS-Fundación Jimenez Diaz (IIS-FJD, UAM), 28040 Madrid, Spain.

[3]Molecular Cytogenetics Group, Human Cancer Genetics Program, Centro Nacional de Investigaciones Oncológicas (CNIO), Melchor Fernandez Almagro, 3, 28029 Madrid, Spain.

[4]Genome Instability and DNA Repair Group, Department of Genetics and Microbiology, Universitat Autònoma de Barcelona, 08193 Barcelona, Spain.

[5]Center for Biomedical Network Research on Rare Diseases, Instituto de Salud Carlos III, Bellaterra, 08193 Barcelona, Spain.

[6]Institute for Transfusion Medicine and Gene Therapy, Medical Center - University of Freiburg, 79106 Freiburg, Germany.

[7]Center for Chronic Immunodeficiency, Medical Center - University of Freiburg, 79106 Freiburg, Germany.

[8]Faculty of Medicine, University of Freiburg, Freiburg, Germany.

[*]Corresponding authors:

Susana Navarro, Telephone: +34913460891. Fax: +34913466484. E-mail: s.navarro@ciemat.es

Juan A. Bueren, Telephone: +34913466518. Fax: +34913466484. E-mail: juan.bueren@ciemat.es

ABSTRACT

The promising ability to genetically modify hematopoietic stem and progenitor cells (HSPCs) by precise gene editing remains challenging due to their sensitivity and poor permissiveness. This represents the first evidence of implementing a gene editing strategy in a murine *safe harbor* locus that phenotypically corrects primary cells derived from a mouse model of Fanconi anemia (FA).

By co-delivering TALENs and a donor therapeutic *FANCA* cassette template to the *Mbs85* locus (ortholog of the h*AAVS1 safe harbor* locus), we achieved efficient gene targeting (23%) in FA mouse embryonic fibroblasts (MEFs). This resulted in the phenotypic correction of these cells, as revealed by the improvement of their hypersensitivity to mitomycinC. Moreover, robust evidence of targeted integration was observed in murine WT and FA-A hematopoietic progenitor cells (HPC) reaching mean targeted integration values of 20.98% and 16.33% respectively, with phenotypic correction of FA HPCs. Overall, our results demonstrate the feasibility of implementing a therapeutic targeted integration strategy in a murine *safe harbor* locus, such as the *Mbs85* gene, of MEFs and murine HPC from a FA mouse model.

INTRODUCTION

Fanconi anemia (FA) is a rare genetic disorder associated with mutations in any of the twenty-two FA genes, known as FANC genes (Bagby, 2018; Knies et al, 2017). The genetic products of these genes belong to a DNA repair pathway known as the FA/BRCA pathway, which is involved in the repair of interstrand cross-link (ICL) lesions during DNA replication. FA patient cells are characterized by the accumulation of DNA damage at an increased rate as compared to healthy cells due to an ineffective FA/BRCA DNA repair pathway. Furthermore, most patients show congenital abnormalities at birth, cancer predisposition (Auerbach, 2009; Schneider et al, 2015; Tischkowitz & Hodgson, 2003), and bone marrow failure (Ceccaldi et al, 2012; Kelly et al, 2007). Due to the risks of allogeneic hematopoietic stem cell transplantation, alternative curative treatments have been proposed. This is the case of gene therapy approaches which aim at the correction of autologous HSPC with therapeutic lentiviral vectors. The efficiency and safety of these strategies in preclinical stages have previously been demonstrated (Becker et al, 2010; Galimi et al, 2002; Gonzalez-Murillo et al, 2010; Jacome et al, 2009; Molina-Estevez et al, 2015; Muller et al, 2008) and are nowadays tested in clinical trials (Adair et al, 2017; Navarro et al, 2015; Tolar et al, 2011; Tolar et al, 2012). However, targeted gene therapy approaches are evolving as a promising alternative to avoid random integration issues arising from the use of retroviral vectors.

Due to the fact that the most frequent complementation group of FA patients is FA-A (60-70%), which is characterized by highly heterogeneous mutations (Casado et al, 2007; Castella et al, 2011) in the *FANCA* gene (Mehta & Tolar, 1993), a therapeutic strategy to precisely integrate a therapeutic *FANCA* expression cassette into a *safe harbor* locus (Papapetrou & Schambach, 2016; Sadelain et al, 2011) would be applicable to all *FANCA* mutations (Diez et al, 2017; Rio et al, 2014) and could be in principle extended to other FA subtypes.

The human *AAVS1* locus located on the first intron of the *MBS85* (*PPP1R12C*) gene on chromosome 19 (Kotin et al, 1992) meets the requirements of a *safe harbor* locus in a wide range of cell types (DeKelver et al, 2010; Hockemeyer et al, 2009; Lombardo et al, 2011; Oceguera-Yanez et al; Ramachandra et al, 2011; Smith et al, 2008; Zou et al, 2011). It has an open chromatin status and also contains a putative insulator element (van Rensburg et al, 2012). Thus, based on the favorable results observed in human cells, we propose to explore a similar strategy in the context of a mouse model of FA-A by integrating a therapeutic *FANCA* expression cassette in the murine *Mbs85 gene,* the ortholog of the human *AAVS1* (Dutheil et al, 2004; Henckaerts & Linden, 2010; Linden et al, 1996a; Linden et al, 1996b) . This gene spans 20 kilobases (kb), and the resulting 3.1 kb mouse cDNA and protein are 77% and 86% identical to their human counterparts, respectively (Tan et al, 2001).

Our study demonstrates the feasibility of conducting a targeted gene therapy approach in embryonic fibroblasts and hematopoietic progenitors from a mouse model of FA-A and highlights the potential of using for the first time the *Mbs85* locus as a murine *safe harbor* for targeted integration, what opens a new platform that allows the study of the real implication of what means a safe harbor locus in an *in vivo* model prior to the clinic.

RESULTS

Targeted genome integration in FA-A mouse embryonic fibroblasts

To establish efficient genome editing at the murine ortholog of the human *AAVS1* gene, we generated a pair of transcription activator-like effector nucleases (TALEN) (Mussolino et al, 2011) targeting the first intron of the murine *Mbs85* gene (**EV1A**). The expression of each TALEN monomer was then evaluated by western blot analyses in HEK-293T cells upon lipofection of the corresponding plasmids using an antibody recognizing the HA-tag (**EV1B**). Mouse embryonic fibroblasts (MEFs) from *Fanca*$^{-/-}$ mice were used to define the optimal conditions for achieving targeted integration at the murine *Mbs85* locus. *Mbs85*-specific TALENs and a donor construct containing a therapeutic human *FANCA* cassette flanked by homologous sequences to the murine *Mbs85* gene (**Fig 1A and B**) were delivered into the FA-A MEFs via nucleofection using different amounts of the *FANCA* therapeutic donor and a fixed dose of TALEN monomers expression plasmids (**Fig 1C)**.

The viability of nucleofected cells was on average around 69% in comparison with 86% of untransfected cells at 48 hours post nucleofection (**Fig 1C**). An *EGFP* control plasmid was nucleofected in these cells as a control to evaluate the transfection efficiency in MEFs, that resulted in 30.17 ± 6.15%. Then, we analyzed the ability of the designed TALEN to disrupt the mouse *Mbs85* locus using Surveyor assay. The frequency of indel mutations ranged from 15% to 36% after nucleofection with these TALENs (**Fig 1D**). The simultaneous delivery of TALENs and donor DNA reduced the frequency of indel mutations by 50%, as compared to delivering the nucleases alone (**Fig 1D,** conditions T+D), suggesting that a number of DSBs were repaired by HR instead of NHEJ.

Once the ability of designed TALENs to cleave the *Mbs85* locus had been corroborated, we evaluated the efficacy of the gene targeting strategy. The presence of a puromycin selection marker in the therapeutic donor allowed us to enrich the population of FA-A MEFs that underwent correct gene targeting. Nucleofected cells were maintained in culture for 5 passages in the presence of puromycin (1-1.25 µg/ml). Diagnostic PCRs were then performed in the bulk population to demonstrate the integration of the therapeutic PGK-h*FANCA* donor into the *Mbs85* locus using the primers indicated to amplify the 5' and the 3' integration junctions (**Fig 1E and Supplementary Table S3**). Samples nucleofected with the TALENs and donor revealed successful gene targeting, with amplification of the specific bands corresponding to the insertion of the donor into the *Mbs85* locus (as shown in **Fig 1E**).

A total of 174 clones were generated by limiting dilution with the aim of determining the efficiency of targeted integration in FA-A MEFs. In two independent experiments, a mean of 23.1% of the clones showed site-specific gene targeting in the *Mbs85* locus, reaching a maximum of 7.4% efficiency at the 5' integration junction. Overall, five clones (nucleofected with 2.5 µg of each TALEN monomer and 0.75 µg of the therapeutic donor) showed the expected 5' and 3´ integration junctions.

Subsequently, we proceeded to determine the frequencies of insertion/deletion (indel) mutations in the FA-MEFs pool by deep sequencing at the on-target site and the 23 putative off-target sites predicted by PROGNOS (Fine et al, 2013) (**Table1 and Supplementary Table1**). The frequency of TALEN-induced indels at the on-target locus of WT and FA-A MEFs was 37.1%, and 30.1%, respectively. These frequencies were also confirmed by Surveyor assay (**EV1C**). Importantly, the frequencies of indels at three identified off-target sites ranged from 0.06% to 0.36%, showing that the used TALENs were highly specific (**Table1 and Supplementary Table 2**). Interestingly, while in WT MEFs we observed deletions with medium lengths of 5 to 9 nucleotides, shorter deletions of 1 to 4 nucleotides were found in FA-A MEFs (**Fig 2**). A more detailed analysis of the different indels generated at the on-target site (**EV2 and 3**) revealed subtle differences between samples of WT or FA-A MEFs, suggesting a potential different repair preference upon nuclease treatment in the two cell types. Furthermore, these analyses revealed that the on-target cleavage predominantly occurred in the range of nucleotides 222 to 226 (**EV4**).

Generation of disease-free and functional FA-A MEF clones corrected by gene targeting in the *Mbs85* locus

Seamless integration of the donor into the *Mbs85* site was validated via Sanger sequencing of the PCR amplicon obtained from the 3' integration junction analysis in one of the five selected clones (Clone #76#, **Fig 3A**). Furthermore, metaphase chromosomes were used to characterize the specific PGK-h*FANCA* transgene integration in chromosome 7 (where the *Mbs85* locus is located) by fluorescence *in situ* hybridization (FISH). We used one probe that recognized the two chromatids of chromosome 7 (which appear as two green spots pointed out by a green arrow in **Fig 3B**), and a second probe that recognized the PGK-h*FANCA* transgene (which appears as a red spot pointed out by a red arrow in **Fig 3B**). Notably, in the two clones analyzed (i.e. #7# and #76#), the red and green signals co-localized in the same metaphase spread, strongly suggesting that the targeted integration correctly occurred at the *Mbs85* locus (**Fig 3B**). However, non-targeted integration events were also observed in some of the metaphase spreads, such as in clone #76# (**Fig 3B**).

To assure the generation of functionally corrected gene-edited FA-A MEF clones we sought to verify whether these clones were functionally corrected in comparison with their parental non-edited FA-A MEFs. First, the functionality of the cassette was tested to determine the expression of hFANCA by Western blot in gene-edited clones. Since mouse MEFs do not express the human FANCA protein, we normalized the expression of hFANCA using a healthy human donor lymphoblastic cell line (HD LCL). As shown in **Fig 3C**, FA-A MEFs, WT MEFs and human FA-A LCLs did not show detectable levels of the hFANCA protein, as expected. However, we observed hFANCA expression both in the bulk population of gene-edited FA-A MEFs (2.5 µg of each TALEN monomer and 0.75 µg of donor) and in clones #7# and #76#. This result demonstrates that our gene-editing approach promoted the expression of the therapeutic h*FANCA* gene in FA-A MEFs upon integration of its expression cassette in the murine *safe harbor Mbs85* locus. As FA cells are characterized by their hypersensitivity to DNA interstrand cross-linking agents, such as mitomycin C (MMC), the sensitivity of uncorrected and gene-edited FA-A MEFs to this drug was tested. Cells were cultured with different doses of MMC and their survival was analyzed at 14 days post-treatment. Selected gene-edited clones

#7# and #76# showed increased MMC resistance as compared to non-gene-edited FA-A MEFs (**Fig 3D**).

The generation of chromosomal breaks upon exposure to DNA cross-linking drugs is another characteristic of FA cells. Thus, to demonstrate the reversion of the characteristic phenotype of FA cells, chromosomal aberrations were studied in edited FA-A MEF clones were studies in the presence and the absence of MMC. Consistent with their restored FA pathway, gene-edited FA-A MEF clones presented a lower number of MMC-induced aberrations per chromosome in comparison with non-corrected FA-A MEFs. Interestingly, the number of chromosomal aberrations per MMC-treated cellwas 10.9-12.1 times lower in edited cells as compared to values obtained in their parental non-edited FA-A MEFs (**Fig 3E**). Altogether these results demonstrate that the specific integration of the therapeutic PGK-h*FANCA* cassette into the murine *safe harbor Mbs85* locus corrects the disease phenotype of FA-A MEFs.

Efficient HDR-mediated gene editing in the mouse *Mbs85* locus of WT HPCs

Our laboratory has previously established an efficient and specific gene editing approach to correct fibroblasts and $CD34^+$ cells from FA-A patients by harnessing the homology directed repair (HDR) pathway to integrate a therapeutic cassette into the human *AAVS1 safe harbor* locus of these cells (Diez et al, 2017; Rio et al, 2014). Experiments shown in Figures 1-3 have shown the feasibility of targeting the mouse ortholog of the human *AAVS1 gene* in mouse FA-A fibroblasts. In the subsequent experiments our goal was to test in mouse HSPCs the therapeutic relevance of the gene editing strategy described above to insert the human *FANCA* donor cassette into the murine *AAVS1* ortholog.

Lineage negative bone marrow (Lin^- BM) cells were purified by cell sorting and then pre-stimulated with a cocktail of hematopoietic cytokines (Navarro et al, 2006; Riviere et al, 2014) for 48 hours to promote cell cycling of quiescent HSPCs. Upon nucleofection with the TALEN and the therapeutic donor described above, pre-stimulated cells were maintained in culture in the presence of hematopoietic growth factors to boost HDR-mediated gene-editing repair (Branzei & Foiani, 2008) until performing the analyses at 48 hours post-nucleofection (**Fig 4A**).

First, the activity of the *Mbs85*-specific TALENs was evaluated by the Surveyor assay in BM-derived Lin^- cells from WT and FA-A mice (**EV5A)**. The cleavage efficacies ranged from 30.4% ± 5.9% to 20.5% ± 10.1% respectively, indicating successful disruption of the target locus in HSPCs from these genotypes (**EV5B**). Since HSPCs are more sensitive to *in vitro* manipulation than adherent MEFs and because limited data are available on effective procedures to nucleofect murine HSPCs (Schiroli et al, 2017), we analysed the survival and transfection efficiency of mouse Lin^- WT BM cells 48 hours after nucleofection with different doses of TALEN plasmids (0.75 µg or 2.5 µg each monomer) and a PGK-*EGFP* reporter donor (2 µg or 4 µg, respectively), flanked by sequences homologous to the murine *Mbs85* locus (**Fig 4B**). A marked reduction (about 7-fold) in the viability of DNA nucleofected samples was observed with respect to untransfected or to mock transfected cells (**Fig 4C**).

When cells were nucleofected with different doses of TALEN and PGK-*EGFP* reporter donor, the percentage of $EGFP^+$ cells at 48 hours post-nucleofection ranged from 11.7% to 27.6% (transient expression), regardless of the TALENs dose. In the absence of the TALENs,

transient expression of EGFP in these cells ranged between 3% and 22% (**Fig 4C**). The ability of nucleofected WT Lin$^-$ BM cells to generate hematopoietic colonies was also evaluated. DNA nucleofection reduced the ability of BM hematopoietic progenitors to generate colonies approximately 9-fold with respect to mock transfected cells (**Fig 4D**).

Although no EGFP-fluorescent colonies were observed in these cultures, we investigated the occurrence of specific integrations of the PGK-EGFP reporter donor into the *Mbs85* locus, by conducting PCRs for the 3' integration junction in hematopoietic colonies. Strikingly, targeted integration (TI) frequencies of 4.8 ± 2.2% were measured in samples nucleofected with 0.75 µg of each TALEN monomer together with the PGK-EGFP donor, and this value increased to 20.9 ± 9.4% when the TALEN dose was increased to 2.5 µg (**Fig 4E**).

Phenotypic correction of gene-edited FA-A HPCs

To prove the therapeutic potential of gene editing in FA-A HSPCs, the *EGFP* reporter donor used in WT cells was replaced with the therapeutic PGK-h*FANCA* donor used in the MEF experiments (**Fig 1 and 3**). Since higher TI frequencies were obtained in WT Lin$^-$ cells using 2.5 µg of each TALEN monomer, we used this dose in subsequent experiments, together with 2 and 4 µg of the PGK-FANCA donor.

Nucleofection of FA-A Lin- BM cells with the TALEN and the donor plasmids reduced the viability of these cells 11-fold either when compared with non-nucleofected or mock nucleofected cells (**Fig 5A**). Similarly, DNA nucleofection also reduced the clonogenic ability of FA-A Lin$^-$ BM cells approximately 9-fold in comparison with cells subjected to nucleofection in the absence of DNA (**Fig 5B**), which is similar to what we observed in nucleofected WT Lin$^-$ BM cells (no significant differences were observed using a two-way ANOVA).

Remarkably, when cells were plated in methylcellulose in the presence or absence of 30 nM MMC, 6% of the hematopoietic colonies corresponding to samples nucleofected with the TALEN and the therapeutic donor survived in the presence of MMC, while only 0.2% of colonies survived in MMC when only the donor was used, indicating that targeting the integration of the therapeutic transgene to *Mbs85* corrected the hypersensitivity of FA HSPCs to MMC (**Fig 5C**). In 16.3% of the colonies that grew in the presence of MMC we confirmed the amplification of the expected Mbs1 3´ integration junction (**Fig 5D**), thereby indicating that correction of MMC-hypersensitivity in primary FA-A mHSPCs was a consequence of the PGK-h*FANCA* targeted integration in the *Mbs85* locus.

DISCUSSION

The *AAVS1* locus has been defined as a bona-fide *safe harbor* locus in humans (Lombardo et al, 2011), in which an exogenous gene could be efficiently expressed in various cell lines and iPSCs (DeKelver et al, 2010; Dreyer et al, 2015; Hockemeyer et al, 2009; Li et al, 2017; Lombardo et al, 2011; Mizutani et al, 2016; Mizutani et al, 2015; Oceguera-Yanez et al; Ordovas et al, 2015; Ramachandra et al, 2011; Smith et al, 2008; Zou et al, 2011). Therefore, in this work, we have decided to carry out a targeted integration strategy in the mouse *Mbs85*

orthologous locus in order to asses if the corresponding mouse locus may serve as a new site where gene editing can be performed in mouse disease models such as Fanconi anemia (FA).

Gene editing of HSPCs is an attractive strategy in FA due to the *in vivo* proliferation advantage of corrected HSPCs over non-corrected ones (Gregory et al, 2001; Gross et al, 2002; Lo Ten Foe et al, 1997; Mankad et al, 2006; Rio et al, 2017; Soulier et al, 2005; Waisfisz et al, 1999). TALEN delivery has remained one of the major obstacles in providing short-term and dose-controllable nuclease activity based on previous studies (Cai et al, 2014; Holkers et al, 2013; Liu et al, 2014; Mock et al, 2014). We nucleofected a pair of TALENs in combination with a homologous donor template, in the form of plasmid DNA, in both MEFs and HSPCs from wt or FA-A mice. Carrying out targeted integration in FA-A cells constitute challenging approaches of gene therapy due to the involvement of the FA proteins in promoting HDR (Adamo et al, 2010; Nakanishi et al, 2005), which could affect the efficiency of the homologous integration of the therapeutic cassette in the targeting site of the genome.

Once the expression of TALEN monomers in HEK293T cells was confirmed (**EV1B**), we established proof of principle for gene editing in FA-A MEFs. Using a stepwise experimental approach as followed in previous gene-targeting studies (Bednarski et al, 2016; Diez et al, 2017; Rahman et al, 2015), we observed relatively high transfection efficiencies (mean value of 30%) and viabilities (ranging from 47% to 78%), indicating that in this cell type cytotoxicity was not a limiting factor to perform gene editing. We also observed that when a donor template was used together with the TALENs, the percentage of repair by NHEJ was significantly reduced; suggesting that a proportion of NHEJ repair was replaced by HDR in the presence of a donor template.

A thorough analysis of the off-target effects is crucial for the further development of gene-editing based therapeutics. We used high-throughput sequencing to assess the off-target sites previously predicted *in silico* with the PROGNOS software (Fine et al, 2013) in nucleofected MEFs, as this method is the preferred one to detect indel mutations induced at low frequencies with great sensitivity (Hendel et al, 2015; Koo et al, 2015). Indels generated by the nucleases were highly specific in WT and FA-A MEFs, as demonstrated by the high percentage of on-target indels and the low percentage of off-target generated indels (**Table 1**). As previously shown for other TALEN (Mussolino et al, 2014; Mussolino et al, 2011), our study confirms the high specificity of the *Mbs85*-specific TALENs.

In some colonies, we had difficulties amplifying the specific PCR bands corresponding for both integration junctions. This could be due to the efficiency of the PCRs, or to the limited and poor quality of the DNA obtained from single colonies. However, as has been previously mentioned, other mechanisms of repair of the DSBs could have been involved apart from HRR, giving rise to different outcomes at the different junctions. Importantly, most of the colonies that arose from samples only nucleofected with the donor did not amplify any of the specific integration bands. In the few cases in which this was observed, on-target non-directed integration events independent of TALEN cleavage may have occurred. We confirmed specific integration of the therapeutic PGK-h*FANCA* cassette into the *Mbs85* locus by PCR when both the donor and the TALENs were nucleofected simultaneously, indicating the generation of HDR-mediated integrations of the therapeutic donor at the on-target site (**Fig 1E**). Importantly,

the specific integration was confirmed by Sanger sequencing (**Fig 3A**) and FISH (**Fig 3B**). However, we also observed the occurrence of non-targeted integration events, highlighting the risks associated with DNA delivery (**Fig 3B,** clone #76#).

In this study, we also confirmed the efficient phenotypic correction of edited MEF cells. This conclusion was deduced both from the functional expression of the hFANCA protein (**Fig 3C**) and the MMC resistance (**Fig 3E**) and reduced MMC-induced chromosomal instability (**Fig 3F**) of edited clones. Taken together, these studies demonstrate the correction of the FA/BRCA pathway through TALEN-mediated targeted integration of a therapeutic h*FANCA* cassette into the *Mbs85* locus of FA-A MEFs.

Once we proved the efficacy of our gene-targeting experiments in FA-A MEFs, we performed similar experiments in mouse HSPCs in order to demonstrate the feasibility of a gene-targeting strategy in the *Mbs85* locus of these cells using the PGK-*EGFP* reporter donor. Working with sorted Lin^- BM cells from WT mice, we observed the expression of the integrated *EGFP* (**EV6**), facilitated by the targeted integration of the *EGFP* cassette into the *Mbs85* locus. Despite the absence of EGFP expression in *Mbs85*-edited WT HSPCs, targeted integration in up to 20.98 ± 9.4% of clones were observed using 2.5 µg of each TALEN monomer together with 4 µg of the *EGFP* reporter donor (**Fig 4E**). This observation and the very low proportion of EGFP-expressing cells observed in liquid cultures suggests a restricted expression of transgenes in the *Mbs85* locus of mHSPCs as has previously been reported in the human *AAVS1* locus of hESCs (Ordovas et al, 2015).

Consistent with the results observed in WT Lin^- BM cells, we demonstrated for the first time the feasibility of conducting a therapeutic gene targeting approach into the *Mbs85* locus of primary Lin^- BM cells from FA-A mice using the PGK-h*FANCA* donor. As for WT mHSCs, both the viability and clonogenic potential of nucleofected FA-A mHSCs (**Fig 5A** and **B**) declined sharply. Regarding the targeted integration observed in WT as compared to FA HSPCs, similar efficacies were observed, supporting the hypothesis that although HDR could be moderately affected in FA-A cells (as was observed in a recent study from our laboratory (Diez et al, 2017)), gene editing is feasible in these cells, due to their mild HDR defects, in comparison with FA-D1 cells.

Of particular importance is the fact that our results show the correction of the MMC-hypersensitivity phenotype in primary FA-A mHPCs. Correctly edited FA-A HPCs survived cytotoxic concentrations of MMC, similarly to what was observed in FA-A MEFs, highlighting the therapeutic potential of the proposed gene therapy approach. Although *Mbs85* might limit the efficacy of expression of integrated cassettes in this locus, the achievement of significant levels of MMC-resistant in edited FA-A CFCs is consistent with our previous observations showing that low levels of FANCA can result in a therapeutic effect (Almarza et al, 2007; Gonzalez-Murillo et al, 2010).

In our studies of DNA nucleofection in mouse HSPCs, we observed a marked cytotoxicity due to transferring plasmid DNA to these cells, as mock nucleofection showed no impairment in viability (**Fig 4D and 4E**). This toxicity that results in a reduction in the efficiency of these strategies, currently constitutes one of the main limitations to conduct *ex vivo* therapeutic approaches of gene editing in hematopoietic diseases (Cornu et al, 2017), however, other

delivery methods might be a safer and overcome this issue (De Ravin et al, 2016; Diez et al, 2017; Mock et al, 2015; Poirot et al, 2015; Qasim et al, 2017; Wang et al, 2015). Nevertheless, our results showing toxicity of gene editing approaches in mouse HPCs are consistent with previous studies aiming at the gene targeting in primary mHPCs (Gundry et al, 2016; Riviere et al, 2014; Schiroli et al, 2017) and confirm that gene editing in the murine HSPC compartment is challenging, particularly in cells capable of hematopoietic repopulation.

Overall, our data provide evidence of successful therapeutic gene editing in the mouse *Mbs85* orthologous locus in fibroblasts and HPCs of a mouse FA model, and establishes the rationale and the proof of principle to use this locus for gene correction in other diseases in preclinical studies to investigate the efficacy and safety of future gene editing strategies.

MATERIALS AND METHODS

Cells and cell culture

HEK-293T (ATCC-CRL-3216™) cells were cultured in DMEM 1X with GlutaMAX™ (Gibco) with 10% Hyclone (GE Healthcare) and 1% Penicillin/Streptomycin (P/S) (Gibco).

MEFs both from FVB/NJ WT and FVB FA-A mice were obtained from the chorion of 13.5 E pregnant females as has been described previously (Navarro et al, 2014). MEFs from WT or FA-A mice were immortalized by a transient transfection with pLXSN 16 *E6E7* and pCL-ECO-gag-pol (Naviaux et al, 1996) using the $CaCl_2$ DNA precipitation method and cultured also in DMEM 1X with GlutaMAX™ (Gibco) with 10% Hyclone (GE Healthcare) and 1% Penicillin/Streptomycin (P/S) (Gibco).

BM cells were isolated from FVB/NJ WT, FVB FA-A or C57BL/6J mice by flushing the femurs and tibias of these mice in IMDM (Gibco). The cellular suspension was incubated with lysis solution ($ClNH_4$ with CO_3HK 1M with EDTA 0.5M) (Merck KGaA) for 5 minutes at RT in darkness. Then, cells were washed with PBS 1X (Sigma® Life Sciences) with 5% Hyclone and 5% P/S. Purified mHPCs, Lin^- (lineage-negative) cells, were obtained by whole BM cell sorting by immunoselection. Lin^- cells were expanded in StemSpan™ (StemCell™ Technologies) with 1% GlutaMAX™ with growth factors and cytokines and 1% P/S. The following factors were added: 100 ng/ml mouse stem cell factor (mSCF), 100 ng/ml human interleukin 11 (hIL-11), 100 ng/ml human FMS-like tyrosine kinase 3 ligand (hFlt3), 100 ng/ml human thrombopoietin (hTPO)(EuroBioSciences).

With the exception of HEK-293T cells that were cultured at standard normoxic (21% O_2-5% CO_2) conditions the rest of the cells were cultured in hypoxia (5% O_2-5% CO_2) at 37ºC, and 95% relative humidity.

TALENs, donors and control plasmids

TALE-based DNA binding domains were assembled using Golden Gate assembly kit (Morbitzer et al, 2011) modified based on our previously optimized TALEN scaffold (Mussolino et al, 2011) (Δ135/+17). The vectors used (Mussolino et al, 2014) included the 17.5th repeat and the wild-

type *Fok*I cleavage domain (pVAX_CMV_TALshuttle(xx); 'xx' stands for the four different 17.5th RVDs used, NI, NG, HD and NN).

Donor plasmids were flanked by two homology arms (HA) of the *Mbs85* locus of 806 bp and 860 bp, respectively. The therapeutic donor contained a PGK.FANCA.E2A.PuroR.SV40pA fragment that was chemically synthesized by GenScript. PGK-*EGFP* reporter donor was cloned in the backbone of the therapeutic cassette by digestion of the PGK.*EGFP* fragment from the pCCL.PGK.*EGFP*.wPRE* plasmid with EcoRI/NotI restriction enzymes (New England Biolabs, Ipswich, Massachusetts, USA). A PGK-h*FANCA* donor with longer homology arms, was used as a positive control for targeted integration in the *Mbs85* locus

Lipofection and nucleofection

HEK-293T cells were lipofected at 70% confluence one day after seeding $1x10^5$ cells with Lipofectamine® 2000 Reagent according to manufacturer's protocol (Invitrogen). 400 ng of DNA of each TALEN monomer were co-transfected with 100 ng of an *EGFP* control plasmid and 500 ng of pUC118 control plasmid.

For nucleofection of WT or FA-A immortalized MEFs, $2x10^6$ cells per condition were used with the Amaxa MEF2 Nucleofector® Kit (Lonza Group) using program T20 of the Nucleofector™ I device, 2.5 μg of each TALEN monomer were nucleofected together with different donor doses (0.75, 2 and 4 μg). Enrichment during 5 passages with puromycin (1-1.25 μg/ml) was performed, then clones were generated by limiting dilution to perform gene targeting studies

For the BM hematopoietic cells, $1.4x10^6$ cells of purified BM Lin^- cells were nucleofected with an *EGFP* control plasmid or the corresponding doses of the TALEN monomers and donors after pre-stimulation during 48h. Lin^- BM cells were nucleofected with the 4-D Nucleofector™ device using the P3 Primary Cell 4D-Nucleofector® X Kit (Lonza Group) kit with the ED-113 program.

Cell sorting & flow cytometry

Lin^- cells were purified from C57BL/6J and FA-A FVB/NJ mice by cell sorting using lineage-specific antibodies phycoerytrin conjugated (BD Pharmingen) (anti-B220 (CD45R), anti-Mac-1 (CD11b), anti-Gr1 (Ly6G/C), anti-CD3-ε, and anti-Tert-119 antibodies) at a concentration of 0.06 μg/mL and 0.02 μg/mL, respectively. For the identification of LSK cells (Lineage negative, $Sca\text{-}1^+$, $c\text{-}Kit^+$), Lin^- cells were stained with the described cocktail, and with 0.06 μg/mL of anti-Sca-1-APC-Cy7 (BioLegend) and 0.15 μg/mL of anti-c-Kit-A647 antibodies (Southern). 4',6-Diamidino-2-phenylindole (DAPI; Roche)-negative staining was used as a marker of cell viability. Analyses were performed in the LSR Fortessa cell analyser (BD/ Becton, Dickinson and Company). Transfection efficiency was also determined by FACS analysis 48h post nucleofection. Off-line analyses were conducted with the FlowJo Software v7.6.5 (© FlowJo, LLC).

Clonogenic -colony forming cell (CFC)- assays of hematopoietic progenitors and colony forming units (CFUs)

CFC assays were performed following manufacturer´s recommendations (Stem Cell Technologies, Vancouver, Canada). MMC (at 10 and 30 nM) (Sigma® Life Sciences) and

puromycin (1 µg/ml) (Sigma® Life Sciences) was added, respectively, to analyze the number of gene-edited cells. $2x10^5$ cells were seeded at 48 hours post-nucleofection. Colonies were scored in an inverted microscope (Olympus IX70 WH10X/22). Cultures were maintained in hypoxia at 37°C, and 95% relative humidity.

Survival of immortalized and targeted FA-MEFs was analyzed by scoring the number of colonies derived from 200 cells (CFUs, colony forming units) exposed to increasing concentrations of MMC (0, 3, 10, 30, 100 and 300 nM). After one week, the medium was changed with fresh medium containing the same concentration of MMC. Cell viability was determined 14 days after cell seeding. All cultures were maintained in hypoxia at 37°C, and 95% relative humidity.

***Cel I* (Surveyor) analysis of TALENs pairs activity.**

DNA was extracted using NucleoSpin® Tissue kit (Macherey-Nagel) from cellular pellets obtained at 48h or after cell expansion. PCR fragments spanning the *Mbs85* TALENs target site were generated with primers mAAVS1 CelIF and mAAVS1 CelIR (**Supplementary Table3**). PCR was performed as follows: 200 ng of gDNA, 1.25 µl 10 µM of each primer, 0.5 µl 100 nM dNTPs, 10 µl of the Buffer 10X and 1 µl of Herculase enzyme (Herculase II Fusion Enzyme, Agilent Technologies) in a final volume of 50 µl. Cycling conditions were the following: 95°C for 2 minutes, 40 cycles of 95°C for 20 seconds, 56°C for 20 seconds and 72°C for 30 seconds, and finally one cycle of 72°C for 3 minutes. PCR products were purified with the NucleoSpin® Gel and PCR Clean-up kit (Macherey Nagel) and amplified following the manufacturer's instructions. Final products were migrated and revealed according to manufacturer instructions and analyzed in a Molecular Imager® GelDoc™ XR+ System (BioRad). Quantification of the bands was performed using the Quantity One Software (BioRad).

On-target integration analyses

Genomic DNA from either the bulk cell population or from FA-A MEF clones was extracted using NucleoSpin® Tissue kit. gDNA from single colonies derived from CFCs assays was extracted as previously described (Charrier et al, 2011). Two PCR reactions were conducted both for the 5' and the 3' integration junctions of the *Mbs85* integration site. To analyze the integration of the PGK-h*FANCA* donor the following primers were used: the pair mAAVS1-5'F (1 & 2) and mAAVS1-5'R (1 & 2); and the pair mAAVS1-3'F (1 & 2) and mAAVS1-3'R (1 & 2) (**Supplementary Table3**). To analyze the integration of the PGK-*EGFP* donor: the pair mAAVS1-5'F3 and mAAVS1-5'R3, and the pair mAAVS1-EGFP-3'F and mAAVS1-EGFP-3'R were used. PCR reactions were conducted using 200 ng of gDNA from bulk cell population or single MEF clones, or 15 µl of gDNA from single colonies. PCRs from the 5' and the 3' integration junctions were performed with 1.25 µl at 10 µM of each primer, 0.5 µl at 100 nM dNTPs, 10 µl of the Buffer 10X and 1 µl of Herculase enzyme in a final volume of 50 µl. Cycling conditions were the following: 95°C for 10 minutes, 40 cycles of 95°C for 30 seconds, 59ºC -mAAVS1-5'F1&R1-; or 58ºC -mAAVS1-5'F2&R2-; or 62ºC -mAAVS1-5'F3&R3- for 60 seconds (for the 5' integration junction depending on the primers used); or 59ºC -mAAVS1-3'F1&R1-; 61ºC -mAAVS1-3'F2&R2-; 62ºC -mAAVS1-EGFP-3'F&R- for 60 seconds (for the 3' integration junction

depending on the primers used); and 72°C for 1.5 minutes; and finally one cycle of 72°C for 10 minutes in a final volume of 50 µl.

PCR products of the 3' integration junction performed in the FA-A MEF bulk population were sequenced by Sanger method. Primers used for sequencing were the followings: mAAVS1-3'-F2, mAAVS1-3'-R2; SeqAAVS1-1_3'_F; SeqAAVS1-2_3'_F; SeqAAVS1-3_3'_F; SeqAAVS1-4_3'_F; SeqAAVS1-1_3'_R (**Supplementary Table3**). Analyses of the sequences were done with Finch TV version 1.4.0 and Vector NTI software.

Fluorescence in situ hybridization (FISH)

Cells were first arrested in metaphase with KaryoMAX Colcemid solution (Gibco) and then harvested after a treatment with a hypotonic salt solution. Two sets of probes were used to localize plasmid integration site. RP23-336p21 and RP24-129K5 specific bacterial artificial chromosomes (BACs) that map to the E3 band of the mouse chromosome 7 (Human BAC Clone Library, Children's Hospital Oakland Research Institute [CHORI]) were used as controls. PGK-h*FANCA* transgene integration site was detected using as probe the DNA from the plasmid vector. Following the manufacturer's specifications, BACs DNA was directly labelled by nick translation (Vysis) with SpectrumGreen-dUTPs, whereas plasmid DNA was labelled with SpectrumOrange-dUTP (Vysis). The probes were blocked with Cot-1 DNA and DNA sheared salmon sperm (Vysis) to suppress repetitive sequences, and hybridized overnight as 37ºC onto metaphase spreads. After post-hybridization washes, the chromosomes were counterstained with DAPI in Vectashield mounting medium (Vector Laboratories). Cells images were captured using a cooled charge-coupled device (CCD) camera (Photometrics SenSys camera) connected to a computer running a Chromofluor image analysis system (CytoVision, Leica Biosystems).

Western Blot

Western blot (WB) analyses were performed to determine the expression of the HA epitope of TALENs in HEK-293T cells using anti-HA antibody (NB600-363, Novus Biologicals). . Human FANCA protein was also analyzed in immortalized FA-A MEFs and in gene-edited FA-A MEFs as previously described (Raya et al, 2009; Rio et al, 2014).

Chromosomal instability assay

Gene-edited FA-A MEFs were subjected to medium containing 40 nM of MMC for 24 hours to induce DNA damage. Then, 0.05 µg/ml of colcemid (KaryoMAX Colcemid Solution, Gibco) was added to the cells followed by treatment with 0.56 % KCl during 15 min at 37°C and fixed in methanol: acetic acid (3:1). Extensions were made at 25ºC with 48% humidity in a Thermotron chamber. Metaphases were stained with 10% Giemsa stain, giemsa's azur eosin methylene blue solution (Merck) with Gibco® Gurr Buffer Tablets (Gibco). Then, cells were placed in glass coverslips with a pair of droplets of Entellan (Merck). In general, a minimum of 20 metaphases per culture were studied for the analysis of aberrations. Cell images were taken with an inverted microscope (Olympus CK30).

Off-target analysis

Possible off-target sites for the TALENs pair targeting the sequences 5'-TGTCCTCTCTTCTTGCTAG and 5'-AGTTACTGGTGGGAACAGA within the mm10 genome were predicted using the online tool PROGNOS (Fine et al, 2013; Lin et al, 2014). In the submitted query, 6 mismatches for each TALEN-half-site and a spacing distance between 10 bp and 30 bp were considered, together with hetero- and homodimeric sites (indicated in **Supplementary Table1**). The 24 top ranked off-targets (TALENv2.0 algorithm from PROGNOS) were analyzed by deep sequencing.

WT and FA-A MEFs were either treated with corresponding nucleases or left untreated. Genomic DNA was isolated to PCR amplify all predicted off-target loci (50 – 100 ng DNA were used per target; primers are listed in **Supplementary Table1**). Libraries were prepared from PCR Amplicons using the NEBNext® Ultra™ II DNA Library Prep Kit for Illumina® (NEB, E7645) and quantified using the ddPCR™ Library Quantification Kit for Illumina TruSeq (biorad, #186-3040). All samples were sequenced on an Illumina MiSeq platform with a MiSeq Reagent Kit v2, 500cycles (Illumina, MS-102-2003).

Paired-end reads from MiSeq reactions were quality trimmed by an average Phred quality (Qscore) greater than 20 using TrimGalor (www.bioinformatics.babraham.ac.uk/projects/trim_galore) and merged into a longer single read with a minimum overlap of 30 nucleotides using Fast Length Adjustment of SHort reads (FLASH)(Magoc & Salzberg, 2011). Merged sequences were aligned against all reference sequences (**Expanded Viev Table 1**) using Burrows-Wheeler Aligner (BWA). Alignments were analyzed for insertions and deletions within a range of ±20 bp of the predicted nuclease cleavage site.

Statistical analyses

Statistical analyses were performed using GraphPad Prism version 5.0 for Windows (GraphPad Software). Results are shown as the mean ± Standard Desviation (SD), mean ± Standard Error of the Mean (S.E.M) in the case of the specific site integration in hematopoietic progenitors, and as the median ± interquartile range, from at least 3 replicates and from different experiments. When two sets of data were compared, two-tailed Student's t-test or Mann-Whitney tests were performed depending on whether or not the values followed a normal distribution. Statistical significance of the indel frequency occurred at predicted off-target sites was determined using a one-tailed, homoscedastic Student's t-test. This test was performed to compare the values that were above those obtained in untreated cells. When more than two sets of data were compared, a parametric one-way ANOVA followed by post-hoc multiple comparison Tukey test or a non-parametric Kruskal-Wallis followed by a post-hoc Dunn's multiple comparison test were used. In some experiments, more than one variable was analyzed. In these cases, when the data suited a normal distribution, the two-way ANOVA test was applied followed by a Bonferroni post-hoc test. Significant differences were indicated as P-value <0.05 (*), P-value <0.01 (**), P-value <0.001 (***) and P-value <0.0001 (****).

ACKNOWLEDGMENTS

This work was supported by grants from the "7th Framework Program European Commission (HEALTH-F5-2012-305421; EUROFANCOLEN)", "Ministerio de Sanidad, Servicios Sociales e Igualdad" (EC11/060 and EC11/550), "Ministerio de Economía, Comercio y Competitividad y Fondo Europeo de Desarrollo Regional (FEDER)" (SAF2015-68073-R), "Fondo de Investigaciones Sanitarias, Instituto de Salud Carlos III" (RD12/0019/0023) and the German Federal Ministry of Education and Research (BMBF-01EO0803). The authors would like to thank Miguel A. Martin for the careful maintenance of NSG mice and Omaira Alberquilla for her technical assistance in flow cytometry. The authors also thank the Fundación Botín for promoting translational research at the Hematopoietic Innovative Therapies Division of the CIEMAT. CIBERER is an initiative of the "Instituto de Salud Carlos III" and "Fondo Europeo de Desarrollo Regional (FEDER)". Finally, although this work was entirely performed with mouse cells, the authors feel deeply grateful to the FA patients and families, clinicians and to Aurora de la Cal as the secretary of the Spanish FA network for always instilling motivation and providing an example for work in this disease.

AUTHOR´S CONTRIBUTION

MJ PB, SN, JB and CM: Conceived and designed the experiments. MJ PB, SN, YG, MV, MH, RSD, SRP,RP: Collection and assembly of data. CM, JS,PR,TC,JB: Provision of reagents, materials, analysis tool, ideas. MJ PB, SN, JB and CM: Manuscript writing.

CONFLICT OF INTEREST

The Division of Hematopoietic Innovative Therapies receives funding from Rocket Pharma. J. A. Bueren is a consultant for Rocket Pharmaceuticals. The rest of the authors declare no competing financial interests.

THE PAPER EXPLAINED

Aim

Despite the success of GT trials that are at present currently undergoing with integrative vectors, gene-targeting approaches represent the next future and are proposed as safer alternatives. These strategies are based on the use of artificial nucleases that generate double strand breaks at specific locations in the genome which can be repaired by the homologous recombination pathway of the cells. Specific sites of the cell genome such as safe harbor locus are being targeted to exploit this approach and facilitate the integration of donor templates that can be therapeutic in the case of genetic diseases.

In this study we aimed at the insertion of reporter and therapeutic donors into the mouse *Mbs85* locus, ortholog of the human *AAVS1 safe harbor* locus using TALEN to investigate the feasibility of targeting a safe harbor locus in the murine context. This strategy was implemented in the *Fanca*$^{-/-}$ (FA-A) mouse model for Fanconi anemia.

Results

We have first demonstrated the activity of designed TALEN to cleave in the *Mbs85* locus of both FA-A embryonic fibroblasts (MEFs) and mouse hematopoietic progenitors cells (mHPCs) from WT and FA-A mice. Targeted integration (TI), as well as evidence of hFANCA expression were shown in gene-edited FA-A MEFs. Moreover, evidence of phenotypic correction was demonstrated in these cells by the reversion of the characteristic hypersensitivity to mitomycin C (MMC), and also by the reduction of the MMC-induced chromosomal aberrations. Gene-editing experiments in WT and FA-A mHPCs also allowed us to demonstrate TI in these cell types. As it was observed in FA-A MEFs, evidence of phenotypic correction was also observed in FA-A hematopoietic colonies. In these experiments, we also observed a marked toxicity of plasmid DNA nucleofection that compromised the repopulating properties of gene-edited mHSPCs in irradiated recipients.

Impact

Our study demonstrates the feasibility of conducting a targeted gene therapy approach in MEFs and HPCs from a mouse model of FA-A and highlights the potential of using for the first time the *Mbs85* locus as a murine *safe harbor* for targeted integration, what opens a new platform that allows the study of the real implication of what means a safe harbor locus in an *in vivo* model prior to the clinic.

FOR MORE INFORMATION

For more information Fanconi anemia research Foundation: www.anemiadefanconi.org and www.fanconi.org

REFERENCES

Adair JE, Sevilla J, Heredia CD, Becker PS, Kiem HP, Bueren J (2017) Lessons Learned from Two Decades of Clinical Trial Experience in Gene Therapy for Fanconi Anemia. Curr Gene Ther 16: 338-348

Adamo A, Collis SJ, Adelman CA, Silva N, Horejsi Z, Ward JD, Martinez-Perez E, Boulton SJ, La Volpe A (2010) Preventing nonhomologous end joining suppresses DNA repair defects of Fanconi anemia. Mol Cell 39: 25-35

Almarza E, Rio P, Meza NW, Aldea M, Agirre X, Guenechea G, Segovia JC, Bueren JA (2007) Characteristics of lentiviral vectors harboring the proximal promoter of the vav proto-oncogene: a weak and efficient promoter for gene therapy. Mol Ther 15: 1487-1494

Auerbach AD (2009) Fanconi anemia and its diagnosis. Mutat Res 668: 4-10

Bagby G (2018) Recent advances in understanding hematopoiesis in Fanconi Anemia. F1000Res 7: 105

Becker PS, Taylor JA, Trobridge GD, Zhao X, Beard BC, Chien S, Adair J, Kohn DB, Wagner JE, Shimamura A et al (2010) Preclinical correction of human Fanconi anemia complementation group A bone marrow cells using a safety-modified lentiviral vector. Gene Ther 17: 1244-1252

Bednarski C, Tomczak K, Vom Hovel B, Weber WM, Cathomen T (2016) Targeted Integration of a Super-Exon into the CFTR Locus Leads to Functional Correction of a Cystic Fibrosis Cell Line Model. PloS one 11: e0161072

Branzei D, Foiani M (2008) Regulation of DNA repair throughout the cell cycle. Nat Rev Mol Cell Biol 9: 297-308

Cai Y, Bak RO, Mikkelsen JG (2014) Targeted genome editing by lentiviral protein transduction of zinc-finger and TAL-effector nucleases. Elife 3: e01911

Casado JA, Callen E, Jacome A, Rio P, Castella M, Lobitz S, Ferro T, Munoz A, Sevilla J, Cantalejo A et al (2007) A comprehensive strategy for the subtyping of Fanconi Anemia patients: conclusions from the Spanish Fanconi Anemia research network. J Med Genet 44: 241-249

Castella M, Pujol R, Callen E, Trujillo JP, Casado JA, Gille H, Lach FP, Auerbach AD, Schindler D, Benitez J et al (2011) Origin, functional role, and clinical impact of Fanconi anemia FANCA mutations. Blood 117: 3759-3769

Ceccaldi R, Parmar K, Mouly E, Delord M, Kim JM, Regairaz M, Pla M, Vasquez N, Zhang QS, Pondarre C et al (2012) Bone marrow failure in Fanconi anemia is triggered by an exacerbated

p53/p21 DNA damage response that impairs hematopoietic stem and progenitor cells. Cell Stem Cell 11: 36-49

Cornu TI, Mussolino C, Cathomen T (2017) Refining strategies to translate genome editing to the clinic. Nat Med 23: 415-423

Charrier S, Ferrand M, Zerbato M, Precigout G, Viornery A, Bucher-Laurent S, Benkhelifa-Ziyyat S, Merten OW, Perea J, Galy A (2011) Quantification of lentiviral vector copy numbers in individual hematopoietic colony-forming cells shows vector dose-dependent effects on the frequency and level of transduction. Gene Ther 18: 479-487

De Ravin SS, Reik A, Liu PQ, Li L, Wu X, Su L, Raley C, Theobald N, Choi U, Song AH et al (2016) Targeted gene addition in human CD34(+) hematopoietic cells for correction of X-linked chronic granulomatous disease. Nat Biotechnol 34: 424-429

DeKelver RC, Choi VM, Moehle EA, Paschon DE, Hockemeyer D, Meijsing SH, Sancak Y, Cui X, Steine EJ, Miller JC et al (2010) Functional genomics, proteomics, and regulatory DNA analysis in isogenic settings using zinc finger nuclease-driven transgenesis into a safe harbor locus in the human genome. Genome Res 20: 1133-1142

Diez B, Genovese P, Roman-Rodriguez FJ, Alvarez L, Schiroli G, Ugalde L, Rodriguez-Perales S, Sevilla J, Diaz de Heredia C, Holmes MC et al (2017) Therapeutic gene editing in CD34+ hematopoietic progenitors from Fanconi anemia patients. EMBO Mol Med

Dreyer AK, Hoffmann D, Lachmann N, Ackermann M, Steinemann D, Timm B, Siler U, Reichenbach J, Grez M, Moritz T et al (2015) TALEN-mediated functional correction of X-linked chronic granulomatous disease in patient-derived induced pluripotent stem cells. Biomaterials 69: 191-200

Dutheil N, Yoon-Robarts M, Ward P, Henckaerts E, Skrabanek L, Berns KI, Campagne F, Linden RM (2004) Characterization of the mouse adeno-associated virus AAVS1 ortholog. J Virol 78: 8917-8921

Fine EJ, Cradick TJ, Zhao CL, Lin Y, Bao G (2013) An online bioinformatics tool predicts zinc finger and TALE nuclease off-target cleavage. Nucleic Acids Res 42: e42

Galimi F, Noll M, Kanazawa Y, Lax T, Chen C, Grompe M, Verma IM (2002) Gene therapy of Fanconi anemia: preclinical efficacy using lentiviral vectors. Blood 100: 2732-2736

Gonzalez-Murillo A, Lozano ML, Alvarez L, Jacome A, Almarza E, Navarro S, Segovia JC, Hanenberg H, Guenechea G, Bueren JA et al (2010) Development of lentiviral vectors with optimized transcriptional activity for the gene therapy of patients with Fanconi anemia. Hum Gene Ther 21: 623-630

Gregory JJ, Jr., Wagner JE, Verlander PC, Levran O, Batish SD, Eide CR, Steffenhagen A, Hirsch B, Auerbach AD (2001) Somatic mosaicism in Fanconi anemia: evidence of genotypic reversion in lymphohematopoietic stem cells. Proc Natl Acad Sci U S A 98: 2532-2537

Gross M, Hanenberg H, Lobitz S, Friedl R, Herterich S, Dietrich R, Gruhn B, Schindler D, Hoehn H (2002) Reverse mosaicism in Fanconi anemia: natural gene therapy via molecular self-correction. Cytogenet Genome Res 98: 126-135

Gundry MC, Brunetti L, Lin A, Mayle AE, Kitano A, Wagner D, Hsu JI, Hoegenauer KA, Rooney CM, Goodell MA et al (2016) Highly Efficient Genome Editing of Murine and Human Hematopoietic Progenitor Cells by CRISPR/Cas9. Cell Rep 17: 1453-1461

Henckaerts E, Linden RM (2010) Adeno-associated virus: a key to the human genome? Future Virol 5: 555-574

Hendel A, Fine EJ, Bao G, Porteus MH (2015) Quantifying on- and off-target genome editing. Trends Biotechnol 33: 132-140

Hockemeyer D, Soldner F, Beard C, Gao Q, Mitalipova M, DeKelver RC, Katibah GE, Amora R, Boydston EA, Zeitler B et al (2009) Efficient targeting of expressed and silent genes in human ESCs and iPSCs using zinc-finger nucleases. Nat Biotechnol 27: 851-857

Holkers M, Maggio I, Liu J, Janssen JM, Miselli F, Mussolino C, Recchia A, Cathomen T, Goncalves MA (2013) Differential integrity of TALE nuclease genes following adenoviral and lentiviral vector gene transfer into human cells. Nucleic Acids Res 41: e63

Jacome A, Navarro S, Rio P, Yanez RM, Gonzalez-Murillo A, Lozano ML, Lamana ML, Sevilla J, Olive T, Diaz-Heredia C et al (2009) Lentiviral-mediated genetic correction of hematopoietic and mesenchymal progenitor cells from Fanconi anemia patients. Mol Ther 17: 1083-1092

Kelly PF, Radtke S, von Kalle C, Balcik B, Bohn K, Mueller R, Schuesler T, Haren M, Reeves L, Cancelas JA et al (2007) Stem cell collection and gene transfer in Fanconi anemia. Mol Ther 15: 211-219

Knies K, Inano S, Ramirez MJ, Ishiai M, Surralles J, Takata M, Schindler D (2017) Biallelic mutations in the ubiquitin ligase RFWD3 cause Fanconi anemia. J Clin Invest 127: 3013-3027

Koo T, Lee J, Kim JS (2015) Measuring and Reducing Off-Target Activities of Programmable Nucleases Including CRISPR-Cas9. Mol Cells 38: 475-481

Kotin RM, Linden RM, Berns KI (1992) Characterization of a preferred site on human chromosome 19q for integration of adeno-associated virus DNA by non-homologous recombination. EMBO J 11: 5071-5078

Li SJ, Luo Y, Zhang LM, Yang W, Zhang GG (2017) Targeted introduction and effective expression of hFIX at the AAVS1 locus in mesenchymal stem cells. Mol Med Rep 15: 1313-1318

Lin Y, Fine EJ, Zheng Z, Antico CJ, Voit RA, Porteus MH, Cradick TJ, Bao G (2014) SAPTA: a new design tool for improving TALE nuclease activity. Nucleic Acids Res 42: e47

Linden RM, Ward P, Giraud C, Winocour E, Berns KI (1996a) Site-specific integration by adeno-associated virus. Proc Natl Acad Sci U S A 93: 11288-11294

Linden RM, Winocour E, Berns KI (1996b) The recombination signals for adeno-associated virus site-specific integration. Proc Natl Acad Sci U S A 93: 7966-7972

Liu J, Gaj T, Patterson JT, Sirk SJ, Barbas CF, 3rd (2014) Cell-penetrating peptide-mediated delivery of TALEN proteins via bioconjugation for genome engineering. PloS one 9: e85755

Lo Ten Foe JR, Kwee ML, Rooimans MA, Oostra AB, Veerman AJ, van Weel M, Pauli RM, Shahidi NT, Dokal I, Roberts I et al (1997) Somatic mosaicism in Fanconi anemia: molecular basis and clinical significance. Eur J Hum Genet 5: 137-148

Lombardo A, Cesana D, Genovese P, Di Stefano B, Provasi E, Colombo DF, Neri M, Magnani Z, Cantore A, Lo Riso P et al (2011) Site-specific integration and tailoring of cassette design for sustainable gene transfer. Nat Methods 8: 861-869

Magoc T, Salzberg SL (2011) FLASH: fast length adjustment of short reads to improve genome assemblies. Bioinformatics 27: 2957-2963

Mankad A, Taniguchi T, Cox B, Akkari Y, Rathbun RK, Lucas L, Bagby G, Olson S, D'Andrea A, Grompe M (2006) Natural gene therapy in monozygotic twins with Fanconi anemia. Blood 107: 3084-3090

Mehta PA, Tolar J (1993) Fanconi Anemia. In GeneReviews(R), Pagon RA, Adam MP, Ardinger HH, Wallace SE, Amemiya A, Bean LJH, Bird TD, Ledbetter N, Mefford HC, Smith RJH et al (eds). Seattle (WA)

Mizutani T, Haga H, Kawabata K (2016) Data set for comparison of cellular dynamics between human AAVS1 locus-modified and wild-type cells. Data Brief 6: 793-798

Mizutani T, Li R, Haga H, Kawabata K (2015) Transgene integration into the human AAVS1 locus enhances myosin II-dependent contractile force by reducing expression of myosin binding subunit 85. Biochem Biophys Res Commun 465: 270-274

Mock U, Machowicz R, Hauber I, Horn S, Abramowski P, Berdien B, Hauber J, Fehse B (2015) mRNA transfection of a novel TAL effector nuclease (TALEN) facilitates efficient knockout of HIV co-receptor CCR5. Nucleic Acids Res 43: 5560-5571

Mock U, Riecken K, Berdien B, Qasim W, Chan E, Cathomen T, Fehse B (2014) Novel lentiviral vectors with mutated reverse transcriptase for mRNA delivery of TALE nucleases. Sci Rep 4: 6409

Molina-Estevez FJ, Nowrouzi A, Lozano ML, Galy A, Charrier S, von Kalle C, Guenechea G, Bueren JA, Schmidt M (2015) Lentiviral-Mediated Gene Therapy in Fanconi Anemia-A Mice Reveals Long-Term Engraftment and Continuous Turnover of Corrected HSCs. Curr Gene Ther 15: 550-562

Morbitzer R, Elsaesser J, Hausner J, Lahaye T (2011) Assembly of custom TALE-type DNA binding domains by modular cloning. Nucleic Acids Res 39: 5790-5799

Muller LU, Milsom MD, Kim MO, Schambach A, Schuesler T, Williams DA (2008) Rapid lentiviral transduction preserves the engraftment potential of Fanca(-/-) hematopoietic stem cells. Mol Ther 16: 1154-1160

Mussolino C, Alzubi J, Fine EJ, Morbitzer R, Cradick TJ, Lahaye T, Bao G, Cathomen T (2014) TALENs facilitate targeted genome editing in human cells with high specificity and low cytotoxicity. Nucleic Acids Res 42: 6762-6773

Mussolino C, Morbitzer R, Lutge F, Dannemann N, Lahaye T, Cathomen T (2011) A novel TALE nuclease scaffold enables high genome editing activity in combination with low toxicity. Nucleic Acids Res 39: 9283-9293

Nakanishi K, Yang YG, Pierce AJ, Taniguchi T, Digweed M, D'Andrea AD, Wang ZQ, Jasin M (2005) Human Fanconi anemia monoubiquitination pathway promotes homologous DNA repair. Proc Natl Acad Sci U S A 102: 1110-1115

Navarro S, Meza NW, Quintana-Bustamante O, Casado JA, Jacome A, McAllister K, Puerto S, Surralles J, Segovia JC, Bueren JA (2006) Hematopoietic dysfunction in a mouse model for Fanconi anemia group D1. Mol Ther 14: 525-535

Navarro S, Moleiro V, Molina-Estevez FJ, Lozano ML, Chinchon R, Almarza E, Quintana-Bustamante O, Mostoslavsky G, Maetzig T, Galla M et al (2014) Generation of iPSCs from genetically corrected Brca2 hypomorphic cells: implications in cell reprogramming and stem cell therapy. Stem Cells 32: 436-446

Navarro S, Rio P, Bueren J (2015) Perspectives on gene therapy for Fanconi anemia. Exper Opinion on Orphan Durgs 3: 1-12

Naviaux RK, Costanzi E, Haas M, Verma IM (1996) The pCL vector system: rapid production of helper-free, high-titer, recombinant retroviruses. J Virol 70: 5701-5705

Oceguera-Yanez F, Kim SI, Matsumoto T, Tan GW, Xiang L, Hatani T, Kondo T, Ikeya M, Yoshida Y, Inoue H et al Engineering the AAVS1 locus for consistent and scalable transgene expression in human iPSCs and their differentiated derivatives. Methods

Ordovas L, Boon R, Pistoni M, Chen Y, Wolfs E, Guo W, Sambathkumar R, Bobis-Wozowicz S, Helsen N, Vanhove J et al (2015) Efficient Recombinase-Mediated Cassette Exchange in hPSCs to Study the Hepatocyte Lineage Reveals AAVS1 Locus-Mediated Transgene Inhibition. Stem Cell Reports 5: 918-931

Papapetrou EP, Schambach A (2016) Gene Insertion Into Genomic Safe Harbors for Human Gene Therapy. Mol Ther 24: 678-684

Poirot L, Philip B, Schiffer-Mannioui C, Le Clerre D, Chion-Sotinel I, Derniame S, Potrel P, Bas C, Lemaire L, Galetto R et al (2015) Multiplex Genome-Edited T-cell Manufacturing Platform for "Off-the-Shelf" Adoptive T-cell Immunotherapies. Cancer Res 75: 3853-3864

Qasim W, Zhan H, Samarasinghe S, Adams S, Amrolia P, Stafford S, Butler K, Rivat C, Wright G, Somana K et al (2017) Molecular remission of infant B-ALL after infusion of universal TALEN gene-edited CAR T cells. Sci Transl Med 9

Rahman SH, Kuehle J, Reimann C, Mlambo T, Alzubi J, Maeder ML, Riedel H, Fisch P, Cantz T, Rudolph C et al (2015) Rescue of DNA-PK Signaling and T-Cell Differentiation by Targeted Genome Editing in a prkdc Deficient iPSC Disease Model. PLoS Genet 11: e1005239

Ramachandra CJ, Shahbazi M, Kwang TW, Choudhury Y, Bak XY, Yang J, Wang S (2011) Efficient recombinase-mediated cassette exchange at the AAVS1 locus in human embryonic stem cells using baculoviral vectors. Nucleic Acids Res 39: e107

Raya A, Rodriguez-Piza I, Guenechea G, Vassena R, Navarro S, Barrero MJ, Consiglio A, Castella M, Rio P, Sleep E et al (2009) Disease-corrected haematopoietic progenitors from Fanconi anaemia induced pluripotent stem cells. Nature 460: 53-59

Rio P, Banos R, Lombardo A, Quintana-Bustamante O, Alvarez L, Garate Z, Genovese P, Almarza E, Valeri A, Diez B et al (2014) Targeted gene therapy and cell reprogramming in Fanconi anemia. EMBO Mol Med 6: 835-848

Rio P, Navarro S, Guenechea G, Sanchez-Dominguez R, Lamana ML, Yanez R, Casado JA, Mehta PA, Pujol MR, Surralles J et al (2017) Engraftment and in vivo proliferation advantage of gene corrected mobilized CD34+ cells from Fanconi anemia patients. Blood

Riviere J, Hauer J, Poirot L, Brochet J, Souque P, Mollier K, Gouble A, Charneau P, Fischer A, Paques F et al (2014) Variable correction of Artemis deficiency by I-Sce1-meganuclease-assisted homologous recombination in murine hematopoietic stem cells. Gene Ther 21: 529-532

Sadelain M, Papapetrou EP, Bushman FD (2011) Safe harbours for the integration of new DNA in the human genome. Nat Rev Cancer 12: 51-58

Schiroli G, Ferrari S, Conway A, Jacob A, Capo V, Albano L, Plati T, Castiello MC, Sanvito F, Gennery AR et al (2017) Preclinical modeling highlights the therapeutic potential of hematopoietic stem cell gene editing for correction of SCID-X1. Sci Transl Med 9

Schneider M, Chandler K, Tischkowitz M, Meyer S (2015) Fanconi anaemia: genetics, molecular biology, and cancer - implications for clinical management in children and adults. Clin Genet 88: 13-24

Smith JR, Maguire S, Davis LA, Alexander M, Yang F, Chandran S, ffrench-Constant C, Pedersen RA (2008) Robust, persistent transgene expression in human embryonic stem cells is achieved with AAVS1-targeted integration. Stem Cells 26: 496-504

Soulier J, Leblanc T, Larghero J, Dastot H, Shimamura A, Guardiola P, Esperou H, Ferry C, Jubert C, Feugeas JP et al (2005) Detection of somatic mosaicism and classification of Fanconi anemia patients by analysis of the FA/BRCA pathway. Blood 105: 1329-1336

Tan I, Ng CH, Lim L, Leung T (2001) Phosphorylation of a novel myosin binding subunit of protein phosphatase 1 reveals a conserved mechanism in the regulation of actin cytoskeleton. J Biol Chem 276: 21209-21216

Tischkowitz MD, Hodgson SV (2003) Fanconi anaemia. J Med Genet 40: 1-10

Tolar J, Adair JE, Antoniou M, Bartholomae CC, Becker PS, Blazar BR, Bueren J, Carroll T, Cavazzana-Calvo M, Clapp DW et al (2011) Stem cell gene therapy for fanconi anemia: report from the 1st international Fanconi anemia gene therapy working group meeting. Mol Ther 19: 1193-1198

Tolar J, Becker PS, Clapp DW, Hanenberg H, de Heredia CD, Kiem HP, Navarro S, Qasba P, Rio P, Schmidt M et al (2012) Gene therapy for Fanconi anemia: one step closer to the clinic. Hum Gene Ther 23: 141-144

van Rensburg R, Beyer I, Yao XY, Wang H, Denisenko O, Li ZY, Russell DW, Miller DG, Gregory P, Holmes M et al (2012) Chromatin structure of two genomic sites for targeted transgene integration in induced pluripotent stem cells and hematopoietic stem cells. Gene Ther 20**:** 201-214

Waisfisz Q, Morgan NV, Savino M, de Winter JP, van Berkel CG, Hoatlin ME, Ianzano L, Gibson RA, Arwert F, Savoia A et al (1999) Spontaneous functional correction of homozygous fanconi anaemia alleles reveals novel mechanistic basis for reverse mosaicism. Nat Genet 22**:** 379-383

Wang J, Exline CM, DeClercq JJ, Llewellyn GN, Hayward SB, Li PW, Shivak DA, Surosky RT, Gregory PD, Holmes MC et al (2015) Homology-driven genome editing in hematopoietic stem and progenitor cells using ZFN mRNA and AAV6 donors. Nat Biotechnol 33**:** 1256-1263

Zou J, Sweeney CL, Chou BK, Choi U, Pan J, Wang H, Dowey SN, Cheng L, Malech HL (2011) Oxidase-deficient neutrophils from X-linked chronic granulomatous disease iPS cells: functional correction by zinc finger nuclease-mediated safe harbor targeting. Blood 117**:** 5561-5572

FIGURE LEGENDS

Fig 1. *Mbs85*-specific TALEN and donor-mediated targeted insertion in FA MEFs. A) Schematic showing the architecture of the murine *Mbs85* locus, with the target sites of the TALENs highlighted, and the structure of the donor used with the therapeutic h*FANCA* cassette driven by the phosphoglycerate kinase promoter (PGK) flanked by sequences homologous to the genomic target locus. The resulting locus upon targeted integration (TI) of the donor is indicated in the lowest part of the panel. mHA-L and mHA-R: homology arms to the murine *Mbs85* locus; 2A: 2A self-cleaving peptide sequence; SV40pA: simian virus 40 polyA sequence; *PuroR*: Puromycin resistance gene. **B)** Flow chart indicating the study design and the different analyses performed in gene-edited cells of FA-A MEFs. **C)** Analysis of viability (percentage of $DAPI^-$ cells) in the different conditions. U: untransfected cells; T: 2.5 µg of each TALEN monomer; D: donor doses (0.75, 2 or 4 µg). Bars indicate the mean ± S.D. (n=2 experiments). **D)** Cleavage efficacy of the *Mbs85*-specific TALENs analysed by Surveyor assay. Representative electrophoresis gel showing the disruption of the target locus in FA-A MEFs nucleofected with only the TALENs (T, 2.5 µg of each TALEN monomer) or together with different donor doses (0.75 µg and 4 µg). U: untransfected cells. Samples not digested with the *Cel1* endonuclease were used as controls. The extent of TALEN cleavage, measured as the mean percentage of modified alleles, is indicated below. Arrows indicate the size of the parental band (405 bp) and the expected positions of the digestion products (224 bp and 181 bp), that are also indicated with asterisks. IX: DNA molecular weight marker. **E)** Schematic representation of the targeted integration of the therapeutic PGK-*hFANCA* donor into the *Mbs85* locus of FA-A MEFs. Arrows represent the primers, forward (Fw) and reverse (Rv) used to evaluate the site-specific integration and the size of the PCR amplicon is indicated for each integration junctions. The electrophoresis gel below is a representative image of the integration analysis performed on the same samples as indicated in C). W: water control; IX: DNA molecular weight marker.

Fig 2. Differential length of nuclease-induced indels in WT vs. FA-A MEFs. All single deletions and insertions at the on-target site were analyzed for their length in nuclease treated WT- and FA-A MEF cells. The percentage of the different deletions or insertions was calculated in respect to all deletions or

insertions respectively. The range shown was reduced to deletions with a maximal length of -30 nt and insertions with a maximal length of 10 nt.

Fig 3. Targeted integration of the therapeutic h*FANCA* donor into the *Mbs85* locus and phenotypic correction of gene-edited FA-A MEF clones #7 and #76#. A) Sequenced region of clone #76# obtained with several primers displaying part of the chromatogram containing the SV40pA sequence, the left and right mHA of the therapeutic cassette, and part of the right location of the *Mbs85* locus (3' integration junction). **B)** FISH analyses in gene-edited FA-A MEF indicating the integration of the therapeutic PGK-hFANCA donor (red spot signal and red arrows) into chromosome 7, (two green signals corresponding to the two chromatids indicated with a green arrow) where the *Mbs85* locus is located. Co-localization of both signals is indicated with an orange circle. DAPI chromosome staining is shown in blue. Scale bar represents 10 µm for all the microphotographs. From left to the right: targeted integration event in clone #7# and targeted and non-targeted integration events in clone #76#. **C)** Western blot analysis of hFANCA expression in the bulk of gene-edited FA-A MEFs, as well as in the gene-edited derived clones. Expression levels were calculated as a fold change with respect to β-ACTIN that was used as a loading control and then normalized against the hFANCA expression of lymphoblastic cells derived from a healthy human donor (HD LCL). FA LCL: lymphoblastic cells derived from a FA-A patient; FA-A: immortalized non-gene-edited FA-A MEFs; WT: immortalized non-gene-edited WT MEFs; FA-AB: bulk of edited FA-A MEFs (T2.5+D0.75). Analysed edited clones: #7# and #76#. **D)** Survival curves after exposure to different concentrations of MMC (0, 3, 10, 30, 100 nM) of edited FA-A MEF clones. In each curve the analysed clone is represented, together with untransfected WT and FA-A MEFs. Star (★) indicates that no colonies were generated in this condition at the corresponding doses of MMC. The survival shown would correspond to the growth of a single colony in these cultures. (**) P-value <0.01, (***) P-value <0.001, (****) P-value <0.0001 indicate significant differences with respect to FA-A group, with a two-way ANOVA followed by a post-hoc Bonferroni test. Asterisks indicate groups with differences (***** WT MEFs; ♦ Clone #76#) with respect to FA-A group. **E)** Chromosomal aberrations per chromosome induced by MMC, analysed in metaphases of gene-edited FA-A MEF clones, in comparison with non-edited WT and FA-A MEFs.

Fig 4. Gene-targeting in WT murine HSPCs. A) Flow chart indicating the study design and the different analyses performed in gene-edited murine HSPCs. **B)** Schematic showing the architecture of the murine *Mbs85* locus, with the target sites of the TALENs highlighted, and the structure of the donor used with the *EGFP* reporter cassette driven by the phosphoglycerate kinase promoter (PGK) flanked by sequences homologous to the genomic target locus. The resulting locus upon targeted integration (TI) of the donor is indicated in the lowest part of the panel. mHA-L and mHA-R: homology arms to the murine *Mbs85* locus; SV40pA: simian virus 40 polyA sequence; **C)** Analysis of viability (percentage of $DAPI^-$ cells) and percentage of $EGFP^+$ cells in WT Lin^- BM cells nucleofected with the TALEN and the PGK-*EGFP* reporter donor at 48 hours post-nucleofection. U: untransfected cells; Double negative (-): Nucleofected without DNA; T: different doses of TALEN monomers (from 0.75 to 2.5 µg); D: 2 or 4 µg of the PGK-*EGFP* reporter donor. Data are the mean ± S.D. (n=5 experiments). (***) P-value <0.001 indicates significant differences with a one-way ANOVA followed by a *post-hoc* Tukey test. **D)** Clonogenic assay to evaluate the ability of WT Lin^- BM cells to generate hematopoietic colonies under the conditions shown in C). Data are the mean ± S.D. (n=5 experiments). (*) P-value <0.05, (**) P-value <0.01 indicate significant differences with a one-way ANOVA followed by a *post-hoc* Tukey test. **E)** Targeted integration percentage of the PGK-*EGFP* reporter donor into the *Mbs85* locus of WT Lin^- BM cells for the 3' integration junction calculated in the hematopoietic colonies that were positive for the PCR. Percentages calculated in nucleofected cells with different doses of TALEN (with triangles, 0.75 µg of each monomer; with circles, 2.5 µg of each monomer) and the donor (in white, the dose of 2 µg; in black, the dose of 4 µg). Data are the median ± interquartile range (n=5-9). (*) P-value <0.05 indicates significant differences with a Mann-Whitney test.

Fig 5. Gene-targeting in FA-A murine HSPCs. A) Analysis of viability (percentage of DAPI$^-$ cells) in FA-A Lin$^-$ BM cells nucleofected with the TALEN and the therapeutic PGK-h*FANCA* donor at 48 hours post-nucleofection. U: untransfected cells; Double negative (-): Nucleofected without DNA; T: 2.5 µg of each NN-TALEN monomer; D: 2 or 4 µg of the therapeutic PGK-h*FANCA* donor. Data are the mean ± S.D. (n=7 experiments). (***) P-value <0.001 indicates significant differences with a one-way ANOVA followed by a *post-hoc* Tukey test. **B)** Clonogenic assays of nucleofected Lin$^-$ cells under the conditions shown in A). Data are the mean ± S.D. (n=7 experiments). (*) P-value <0.05 indicate significant differences with a one-way ANOVA followed by a *post-hoc* Tukey test. **C)** Phenotypic correction measured with clonogenic assays in nucleofected FA-A Lin$^-$ BM cells treated with 30 nM MMC compared to cells cultured in the absence of MMC. MMC survivals are indicated considering the number of hematopoietic colonies generated without drug selection as 100%. Cells were subjected to nucleofection with 2.5 µg of each TALEN monomer and the therapeutic PGK-h*FANCA* donor (2 and 4 µg). Data are presented as mean ± S.D. (n=4 with the except of D2 µg where n=1 experiments). No statistical differences were found among groups with a non-parametric Kruskal-Wallis and median test. **D)** Representative PCR analysis for the study of the 3' integration junction (1,337 bp). C+: sequenced genomic DNA positive for the integration junction in edited FA-A MEFs; T+D: samples from nucleofected FA Lin$^-$ BM cells with 2.5 µg of each TALEN monomer together with 4 µg of the therapeutic PGK-h*FANCA* donor; D: 4 µg of the therapeutic PGK-h*FANCA* donor; IX and λ BstII: DNA molecular weight markers. Analysed colonies are numbered and the positive ones framed in blue.

TABLES AND THEIR LEGENDS

ID	Closest Gene	Region	Chromosomal coordinates[1]	Match Type	mismatches		Left Target (5'-->3`)	Spacer (bp)	Right Target (3'-->5`)	WT MEFs			FA-A MEFs		
					Left	Right				indel frequency nuclease treated	indel frequency untreated	p-value[2]	indel frequency nuclease treated	indel frequency untreated	p-value[2]
1	Mbs85/Ppp1r12c	Intron	chr7:44999244499974	R13L	0	0	TCTGTTCCCACCAGTAACT	13	GATCGTTCTTCTCTCCTGT	37.12%	0.10%	**<0.0001**	30.15%	0.04%	**<0.0001**
2	Vstm2b	Intron	chr7:40912153-40912210	R20L	3	6	TCTGTaCCCcCCAGaAACT	20	GgTCtcTCTcCTCTCCctT	0.08%	0.07%	0.3607	0.14%	0.12%	0.0524
3	Gcnt4	Intergenic	chr13:96885014-96885067	L16R	4	4	TGaCCTCcCTcCTTGCTAa	16	aaAATGACgACaCTTGTCT	0.07%	0.11%	0.9925	0.06%	0.08%	0.8157
4	Opcml	Intron	chr9:28002385-28002449	L27L	3	5	TGTCCTCTCTTCcTcaTAG	27	GATCGgTgTTCTaaCCgGT	0.08%	0.07%	0.261	0.07%	0.08%	0.6144
5	Ush2a	Intron	chr1:188788167-188788219	L15R	4	4	TcTCCTCTCTTCTTcCcAt	15	aaAATGACgACaCTTGTCT	0.11%	0.19%	1	0.12%	0.16%	0.9931
6	Hs3st3b1	Intergenic	chr11:63609864-63609925	L24R	6	3	TGTCtTCTCTgaTTGgTta	24	TCAATGACCcCtCTTaTCT	0.07%	0.07%	0.3805	0.08%	0.07%	0.0729
7	Gm15800	Intron	chr5:121256750-121256814	R27L	6	3	gCTtTTCCCcCCAGcAgCc	27	GATCGgTCgTCaCTCCTGT	0.05%	0.06%	0.7362	0.06%	0.07%	0.8889
8	Pga5	Promoter	chr19:10678302-10678365	R26R	5	4	TCaGaTCCCACCAGctcCT	26	cCAAcGACCgtCCTTGTCT	0.06%	0.05%	0.0711	0.06%	0.05%	0.3296
9	4933402J15Rik	Intergenic	chr14:74102062-74102121	L22R	6	4	TtTaCTCTCTcCTTaCTca	22	aCAAaGACCAaCCTcGTCT	0.09%	0.09%	0.7021	0.09%	0.08%	0.154
10	Odz4	Intergenic	chr7:95688609-95688671	L25R	6	3	TGTCCcCTCTTCTTttaca	25	TCAATccCCACCtTTGTCT	0.06%	0.06%	0.532	0.06%	0.06%	0.3905

11	Acbd6	Intron	chr1:155609313-155609377	L27L	4	6	TaaCCaCTCTTCTTGCTAa	27	GgTgGTTtcTCaCTCCaGT	0.09%	0.09%	0.251	0.09%	0.08%	0.1802
12	Nkx6-1	Intergenic	chr5:101585362-101585421	R22L	4	5	TCTGTTCaCAgCAGTAAaa	22	GATCGTTaaTCTtTaCTaT	0.12%	0.15%	0.9362	0.14%	0.16%	0.9359
13	Adam32	Intron	chr8:24878909-24878961	R15L	6	4	TCTaTctCCACtAtTAcCT	15	GATCaTTCaTCatTCCTGT	0.36%	0.09%	**<0.0001**	0.33%	0.11%	**<0.0001**
14	Cdh11	Intergenic	chr8:102833188-102833235	R10R	6	3	TCTGTaaCCtagAaTAACT	10	TCgtTGACtACCCTTGTCT	0.06%	0.07%	0.9009	0.08%	0.06%	**0.0195**
15	Gm5072	Intergenic	chrX:91403414-91403472	L21R	5	4	TGTaCTCTtTgCTTGgTgG	21	TCAATGACCAaCCaaGTaT	18.37%	19.34%	1	17.00%	18.10%	1
16	Cry1	Intergenic	chr10:85202507-85202573	R29L	4	5	TCTGTaCaCACCAcTcACT	29	GtTCGaTtTTCTCTCCcGa	0.14%	0.14%	0.5045	0.13%	0.13%	0.4995
17	Il20ra	Intron	chr10:19752347-19752396	L12L	4	5	TtTCCTCTtTTCTTtCaAG	12	GATCcTTtTcCTCTCCTca	0.11%	0.08%	0.0559	0.07%	0.12%	0.998
18	Sec11c	Intergenic	chr18:65798262-65798317	R18R	5	4	TCTGTcCaCAaCAGTAtaT	18	aaAATGACgACaCTTGTCT	0.06%	0.07%	0.7833	0.08%	0.07%	0.4279
19	Tmem132b	Intergenic	chr5:126222277-126222336	L22R	6	4	TaTCCaCTCaTCTTtCaAt	22	TCAATGAtgACaCTTaTCT	PCR failure					
20	Atp6v1h	Intergenic	chr1:5298497-5298562	L28R	4	4	TGTagTtTCTTCTTGCTgG	28	TCAActACCACCCTTGgtT	PCR failure					
21	Rab2a	Intergenic	chr4:8505300-8505349	R12R	6	4	TtTtTTCCCAaaAaTAACa	12	aCcATGACCACCCgTGTaT	0.24%	0.18%	**0.0034**	0.19%	0.17%	0.1491
22	Luc7l	Exon	chr17:26254092-26254159	R30L	3	6	TtTtTTCCCACaAGTAACT	30	agTCaTTtTTCTgTgCTGT	0.10%	0.23%	1	0.12%	0.12%	0.5934
23	Akr1b7	Intron	chr6:34420642-34420698	L19L	4	6	TGTCtTCcCTTCTTcCaAG	19	GATCtTTCgaCcCTaCTGa	0.05%	0.05%	0.4947	0.04%	0.05%	0.5552
24	Pvt1	Intergenic	chr15:62406674-62406723	L12R	6	4	TGTCCTtaCTTCagGaTgG	12	aaAATGACaACaCTTGTCT	0.12%	0.11%	0.3355	0.10%	0.11%	0.7653

[1] Chromosomal coordinates are based on the mm10 genome, [2] In bold the sites with a statistically significant differences as compared to controls ($p<0.05$).

Table 1. Off-target cleavage of Mbs85-specific TALENs. The top off-targets are listed according to the ranking generated with TALENv.2 algorithm from PROGNOS software. The nucleotide differences in the left and in the right targets, the closest gene, the region and chromosomal coordinates of the off-target location are indicated. The match type and the sequence of the left and the right target are also included. The indel frequency and p-value are also indicated.

EXPANDED VIEW FIGURE LEGENDS

Expanded View Figure 1. Efficient TALEN-mediated editing of *Mbs85* locus. A) Schematic representation of the *Mbs85* genomic locus (Chromosome 7: 4,481,520-4,501,680) and the TALEN-targeted sequences (intron 1). The TALEN backbone contains an N-terminal NLS, the '0 repeat' , the 17.5 'half-repeat'. This is followed bythe C-terminal domain fused to the catalytic *FokI* cleavage domain, as shown in panel B) The amino acids sequence of the DNA binding modules of the engineered TALENs (represented with different colors according to the cipher NG = T, HD = C, NI = A and NN = G or A), as well as the expected target sequences are indicated. **B)** Evaluation of TALEN expression in HEK-293T cells by WB analysis using an antibody directed against the HA-tag present in each TALEN monomer. **C)** Evaluation of the cleavage efficacy of the *Mbs85*-specific TALEN pair using the mismatch sensitive Surveyor assay in WT and FA-A MEFs. Representative electrophoresis gel showing the frequency of indels (calculated as the mean percentage of modified alleles) at the target locus using 2.5 μg of each TALEN monomer. Arrows indicate the size of the parental band (405 bp) and the expected positions of the digestion products (224 bp and 181 bp), that are also indicated with asterisks. ϕ: transfected cells without DNA (mock condition); IX: DNA molecular weight marker.

Expanded View Figure 2: Differential repair preference leading to insertions in WT and FA-A MEFs upon nuclease treatment. Positions of insertions and respective sequences identified at the on-target site. The 24 top most insertions in the on-target locus are shown in **A**) as alignment to the reference sequence, and highlighted in bold and in **B**) as percentage of all insertions comparing WT-MEFs to their respective counterparts FA-A MEFs. Nucleotide positions refer to the amplicon sequence provided in Supplementary Table1.

Expanded View Figure 3: Differential repair preference leading to deletions in WT and FA-A MEFs upon nuclease treatment. For all single deletions, the deleted regions and sequences identified at the on-target site. The 24 top most deletions in the on-target locus are shown in a) as alignment to the reference sequence and in b) as percentage of all deletions comparing WT-MEFs to their respective counterparts FA-A MEFs. Percentages of individual deletions were calculated in respect to all deletions. Nucleotide positions refer to the amplicon sequence provided in Supplementary Table1.

Expanded View Figure 4. On-target cleavage predominantly occurs in the range of nucleotide 222 to 226. The deletion frequencies of each single nucleotide were calculated as percent of the total reads showing an indel in the analyzed on-target region. Nucleotide positions refer to the amplicon sequence provided in Supplementary Table1.

Expanded View Figure 5. Evaluation of cleavage efficacy of TALEN in the *Mbs85* locus of WT and FA-A Lin$^-$ BM cells by Surveyor assay. A) Representative electrophoresis gel showing the disruption of the target locus using 2.5 μg of each TALEN monomer indicated as T. The extent of cleavage measured as the mean percentage of modified alleles is indicated below the image. Arrows indicate the size of the parental band (405 bp) and the expected positions of the digestion products (224 bp and 181 bp), that are also indicated with asterisks. U: untransfected cells; IX: DNA molecular weight marker. **B)** Histogram representing the percentage of cleavage monitored with the Surveyor Assay in WT and FA-A hematopoietic progenitors. Bars indicate the mean ± SD (n=3 experiments in WT cells and n=4

experiments in FA-A cells). No statistical differences between groups was observed using a Student's t-test.

Expanded View Figure 6. Evaluation of the efficiency of EGFP expression of WT Lin$^-$ BM cells nucleofected with the TALEN and the PGK-*EGFP* reporter donor at 2 and 14 days post-nucleofection. A) Representative flow cytometry dot plots of EGFP$^+$ cells analysed at day 2 and 14 post-nucleofection of WT Lin$^-$ BM cells. T+D: 0.75 or 2.5 µg of each TALEN monomer together with 4 µg of the PGK-*EGFP* reporter donor; D: 4 µg of the PGK-*EGFP* reporter donor. EGFP$^+$ expression was determined discarding autofluorescent cells (576/26 channel). **B)** Representative image in liquid culture of EGFP$^+$ Lin$^-$ BM cells at 14 days post-nucleofection. EGFP$^+$ fluorescent cells could be observed in the microscope in T+D conditions. Scale bar represents 50 µm for all the microphotographs. **C)** Geometric Mean Fluorescent Intensity (measured in arbitrary units, a.u.) of nucleofected cells analysed in the same conditions shown in A). Data show the mean ± S.D. (n=2-3 experiments). Statistical analysis could not be performed.

EXPANDED VIEW TABLES AND THEIR LEGENDS

ID	Closest Gene	TALEN Score	Forward Primer	Reverse Primer	Amplicon length	Predicted cleavage site	Amplicon Sequence
1	Mbs85/ Ppp1r12c	100	GGACGGAT GGATTCTGG GTG	GGGTTC TTCTGG ATTCAG GATGC	405	225	TCACCTTGCTTCCACTTTCCAAGCCCCTGGTTTCCTGA GCTCTAAGTACCCACTCTACCACCCAAGCTACATCGC AGCCCAGGACGGATGGATTCTGGGTGTTTTTTCTCTA CCTGCAAGTGTGAAAATTGAACCTGTCAAATACCCTC GCTCTGTTTCCCATCTCCACAGGCAGCAGGCGTCCCT TCCAGGATCCCCTCTGTTCCCACCAGTAACTGAACTA CGGGATCCTAGCAAGAAGAGAGGACAACCCAGGAG ATGGAAGTTGCCATGAAAGAAGCTGCCCACCAGAAG ACTGACATTGGACCAACACTGAGACCAGGAGGGAGA ACTGGGATGTAGGCTCTTGTGTGACTTATCTTGTTCT CGGTCATCCTAACTGAATAAAAGCATCCTGAATCCAG A
2	Vstm2b	56.69	GGCCAGAG GGAAGTTCA ACTAC	GGATGG CGTGAA GATGAG GAC	369	234	GGCCAGAGGGAAGTTCAACTACTTTTCTACACAAGA ATTCTCCTTTCAAATACACCAGTAATGCCTGTTGTGTT TGAAGTTACCACTAGACTTTCTTTGGAAATTCAAAGA TGATTTGGACAGGATACCTGACCAAGCACTGAGAAG TTTAAGATAACCACAAAAGTATAAAGGAGAGGGAGA ACACTCGAGTTAGAGGACAGTCTGTACCCCCCAGAA ACTCATTGTAGAGACACTAGAGCCCAGAGAGAGGAG AGGGAAAGGACAAGGGAAGGAGAGCATCAGACCCT CAGAGAGAGGAGAGGGAAAGGACAAGGGGAAGGA GAGCATCAGACCCTGATCCTGCTAGTCCTCATCTTCA CGCCATCC
3	Gcnt4	55.89	GTCTCTTGG ACTACCCTG ACTAAC	CTGAAT AGATAC TGCCAT GCTCCC	292	156	GTCTCTTGGACTACCCTGACTAACAACTCAAAAAGA GGTTTCATTCAAGGTGTGTGTGTGTGTGTGTGTGTGT GTGTGTGTGTGTGTGTGTGTGTGTTACTCATTCCCAC TCCTTTTCTTTCTGTATTGACCTCCCTCCTTGCTAAGCT GTCTTAGTTAGGGTTTTACTGCTGTGAACAGACACCA TGACCAAGGCAAGTCTTATAAAAACAACATTTAATTG GGGCTGGCTTACAGGTTCAGAGGTTAAGTCCATTATC ATCAAGGTGGGAGCATGGCAGTATCTATTCAG
4	Opcml	55.47	GTTTTTGTTC CCTGACACC CTGAG	GACTCT GCCAGG TGCACT GT	283	147	GTTTTTGTTCCCTGACACCCTGAGTTATTATCATAGT GGTGGCAGATACTGTTACCTAGGTCTTAGCAAGGCA AAGGCTGATAGGTGAGAAAGAGACTTACGTGGTTTC CTGGTGTCCTCTCTTCCTCATAGGAAAGTGGATCTCTT TCTTTGTGTTAGCTAGCCACAAGATTGGCCATAGCCT CAACCTAAAGCCAGCCTCGTCTGCTCTCATCACATCC AGAGAATATGGCCAGACACAGAGCCCCACAAAACCC TTTTGGACAGTGCACCTGGCAGAGTC
5	Ush2a	55.04	CAGGGGAC AACTTTTGA GTGTCCA	CTCAGCT CCTCCTG CACCAT	295	150	CAGGGGACAACTTTTGAGTGTCCATTCTTAGTTCTCT GCAGATTGATGCAGGGTCTCTCCCTTTTCTGTCACCCC ATAGCATACTCCAGGATAGGTGGCCCATCAGCTTCTG GCCAAGTCTCTCTCCTCTCTTCTTCCCATCTGTCTTAG GTAGGGTTTTACTGCTGTGAACAGACACCATGACCAA GGCAAGTCATTTAATTGGGGCTGGCTTACAGGTTCA GAGATTCAGTCCATTATCTTCAAGGTGGGAGCATGG CAGTATCCAGGCAGGCATGGTGCAGGAGGAGCTGA G
6	Hs3st3b1	54.7	GGAGCATTT TTGGTGCTG CTGTG	CCCATCA CATCTTA GAGAGA CCC	278	143	GGAGCATTTTTGGTGCTGCTGTGTATTCAAAGGCTA AGTACCAGCCCCCCATAATCTGTGTGCCCCTTGAACA GATCCTCAGGTACACCGAGTGAGGGGTAAACGGTCC TTGTCTTCTCTGATTGGTTAAATACACAGATGTGGCT GACAGCCAGTTACTGGGGAGAATAGAGGTAGGTGA GGCTAGGTTCCTGGGCTCAGCGTCCTAGGTAGGGAC CACAAGGAGAGAAGGAGGAGGAAGAAGAAAGAGG AAGGGGGTCTCTCTAAGATGTGATGGG
7	Gm15800	54.44	CCCTCTCCA GCAGTTATG CC	GGAACA AAGCTG AGATGG GACAAG	274	136	CCCTCTCCAGCAGTTATGCCATTATTGCACCAGTGAG GACCATCCTGCCTGGCAGGTGAGTAGGGTGTGCTTA GGCTTCACAGCTGGATGGGACTGTTGATGGCTTTTCC CCCCAGCAGCCCACCTGGTACTGCCAGCACTGTGAAA GCTAGCCAGCAGTGAGGACACTTCCAGTTTCTCCTGC ATTTGGGGGAGAGAGTGTGTGTGTCTCCCTATGT AAGCCAGGGACGTCAGGGAAGGAGACCATGCTTGTC CCATCTCAGCTTTGTTCC
8	Pga5	54.24	GGTAGCACC AAGTCACCT GATTTC	GCAAGG ACTAGC TGCCTAT CTTC	**381**	144	GGTAGCACCAAGTCACCTGATTTCACAGAGTGGAGA GACTCTTGCTATCTTGGTGATAAAGACACTGTGGATA AAGTGACAAAGGTAAGTGCCAGGTGCCTCTCTGCTG GTCAGATCCCACCAGCTCCTCACTGGCCTGTCCTCATT AGAGAGTGGGTTGCTGGCAGGAACAGAAGGCCGAG TCTGACAACCTGAGTTTGATAGCCAGGGCCAAGTTTA ACCTCCATACACCTCTGTGGTAGAGGCACCCACCCAC CCACATCAAACAAACAAACACATAAATACAACAGTAA ATGTAAAATGTATCCATGATAAGTGGAAGACTTTTAA AAAGTTTATTTTTCTTTAAAAACCAAAAGAAGATAGG

							CAGCTAGTCCTTGC
9	4933402J15Rik	54.16	CTCATGAGTTTCTGGGAGAGGTAG	CCACTGTGGATGATGCTTCCTAAC	**395**	224	CTCATGAGTTTCTGGGAGAGGTAGAAAAGTAGTCCCTAAAAGTTAAGCTTTCAAAAGCAACAGTGAAAGCTATGTTGCAAAGTAACCTAAAAAGGTGTCAGCTGTTGCTGTAGCTACCTGTCTGTGATTAGTGCTTCTATAGCTAGAGTCTTCTACTGACATCTCTGCTACCAACGCAGATGCTCAAAAAGCTTTACTCTCTCCTTACTCAAACAGTGGAAATCCCATGTAGGTGTTTCTGGTTGGAGCAGAAATAGCATGGAGACCTAGAAAATCATAACAGTGTAAGAAGGATGTTCATTGCGTTAGTCATATAAGCCAGGTGTTCACACATGTCTTTGTAAAACTATCGAGATTGTCAAATGAGTTGTGTTAGGAAGCATCATCCACAGTGG
10	Odz4	53.96	CAGAGTGCTCCTCAACCTGC	CACACAAAGCTCAGCCTGAAGAC	308	137	CAGAGTGCTCCTCAACCTGCTCCACTGCCCTGCATTCACAGCTAGCCATCACCCCTCCACCCCCCAACACCAAGTGAATGAATCGAAACCTTGGGTAAGGGGAATGTCCCCTCTTCTTTTACATTTGAACTCAGCATCAATTTCATCCAGTTAGGGGTGGAAACAGAAAACCGAAAAGAAAAGAGAGAGAGGGACTCACCAGGATGTTGAATGGGCAAAAGAAGAAAGAATAGAAAGAAAGAAGGAAAGAAAAAGAAATCTCTCAAAAGGCACTTTTATTTCATTGTCTTCAGGCTGAGCTTTGTGTG
11	Acbd6	53.45	CTGCCGTGCAGTAGCTTTCTAG	CCATGTTCCCCACCGTAACTG	**341**	140	CTGCCGTGCAGTAGCTTTCTAGAATATGTTCCTCCAGTGTAACCAAACTTTGTTGCTTTAACCAACATCTTTGTTTCTGACCTGTCCTCCCTCTTCTAGTCTGAGGTAACCACTCTTCTTGCTAAATTGATGTGAAGTGTACCTTTAAGAATCCACCAAAGAGTGAGGTCATACAGTGTCCTTCTGTGTTAGACTTCTTTCCCGCGTCATAGTGTCTTACATACGGCTCTATTGCTGTGAAGAGACACCATGACCAAGGCAACTTATAGAAGAAAACATTTAAATGAGGTTTACAGTTTCAGATGATGAGTCTACTATTACAGTTACGGTGGGGAACATGG
12	Nkx6-1	53.39	CCGCTGCCATAACTCAGCCT	GGGATGGGAGGTGAATATGTCCAA	**353**	140	CCGCTGCCATAACTCAGCCTTGATGATAATAATGAACTGAACCTCTGAACCTGTAAGCCAGCCCCAATTAAATGTGGCCCTTATAAAAGACTTGCCTTAATCATGGTGTCTGTTCACAGCAGTAAAACCCTAACTAAGACAGGTTGTTTCTAGCAATTAGAAATGATATTATTTCTATGGTAGCCATCAGTAATGAGCAAACATCTTAATTATTGTTCTGCTGTGTCAACTGATTCTGAAAACGATCATTTTGTCTTAGTATTCATTGTGTGTGTAATATTGTTATTCTACATGTATATAGAATAACATAATACATATGATAATTTATTTTGGACATATTCACCTCCCATCCC
13	Adam32	53.38	CCCTGGATTTCTTCATAGCAGGC	GCCTTGTGCTCTACATACACATCC	289	150	CCCTGGATTTCTTCATAGCAGGCAAATGGAGCATTCACTGAACCTATCAAAATTAGAAACATATTTAGATTAGATTATATATTTGTGCTTCTCCATGTCCTCATACACCATGCTTCCTTACCTCTATCTCCACTATTACCTAACTCAAAAGGTTTTCTAGTAAGTAGTAAGGACAGAGAAAGAACTTTCATGACTATGATGTAATGCTACTTTGCTACATTGTATTCATTTCTGTAACATAAAATACAAGAGAAAGGAGAGTTATGGATGTGTATGTAGAGCACAAGGC
14	Cdh11	52.96	GGCAGGGCTAAAGACAGAGCA	CTCTGTGAAGCCTGGTGAGTTCAA	**320**	152	GGCAGGGCTAAAGACAGAGCAAAATTTGAGAACTTGGTCAACCAATGACTGACTCAGCTTGAGCTCCATGCCATGAGATGGAGATCACCCCTGACACTGTTAATGACACCCCTGCTATATTTGCAGTCTGTAACCTAGAATAACTGGGTTCATCCAGCAACTGATGGGAACAGATACAGAGAACTACAGCCAACCATTAGGCAGAGCTTGGAGCATCCTTCAGAAGAAGGGGAAGAAGGATTGTAGGGGCTAGAGGAGTCAAGGACAACACAAGTATACTTACAGAATTGACTAATTTGAACTCACCAGGCTTCACAGAG
15	Gm5072	52.87	GTGGAGCAGAGAGCCTTCACA	GGATGCTCTCAGCCAACCATTGAA	271	135	GTGGAGCAGAGAGCCTTCACAGGACCAAGGACCACTCCTCCCATTGATGTCCAAGAAGGCCATCCTCTACTACATATGCGGCTAGAGACATGGGTCCCTCCATGTGTACTCTTTGCTTGGTGGTTTAGTCCCTGGGAGCTCTGGAGTTACTGGTTGGTTCATAATGTTGTTCCTCCTATAGGGCTGCAAAACCCTTCAGCTCCTTAGGTCCTTTCTCTAACTCCTCCATTGGGGACCCTGTGATCAGTTCAATGGTTGGCTGAGAGCATCC
16	Cry1	52.82	CCCCCCCTTTTTAGAATGTACTGC	TCCCAGTCTTCCTTCTTGAACCC	301	165	CCCCCCCTTTTTAGAATGTACTGCTAGATTTATCAACAGAATAAGAAGATCAATCTCTTGAGGCTTACAAGAGAGACTGCAGTTTACATTTCCCCACTGCAATGCATCGAACGGAAGTTTAAAGGTGATCTCTGTACACACCACTCACTTCCCAGCCCCTTTTCCTTCTCACAGACAGCAAGCTAAAAGAGAGGGCTGTAAGTTCTTTCCTCCCTAAGAGTGTTCATTTTCAGCAGAATTGGCAAAGAGGGGGGAACCCTGCTTGCAATGCAATCTGAGGGTTCAAGAAGGAAGACTGGGA
17	Il20ra	52.81	AACCCACAGTCCCAGCTCCA	CCTTCCCTGCTTGCTTGGTATTTG	285	136	AACCCACAGTCCCAGCTCCACCCCCACCCGTCTCAACTGCACCCCTGCCACAACCCCACTCCCACCCCAGCCCCAGCCTCACCCCTATCCCCACCCCTTCCCACTCTACTTTCCTCTTTTCTTTCAAGTTGAAACAGTCCCTAGGAAAAGGAGAGGAGTGTTGGAAACACATTTGAACAAGGAAAAGCTTTCCTTCTGAGTTACTTTATCATGCCGTCTCTTTG

							AAAAGAAAGCATTCTCTACCATAATGCAAATAAAACTCAAATACCAAGCAAGCAGGGAAGG
18	Sec11c	52.77	AGGCACACCGTGAGCCTACA	CTACCTGGATACTGCCATGCTC	272	137	AGGCACACCGTGAGCCTACAGGTGGTGGGGCTGGCAGAAGCATCAGGGACAGGAAGGCAAATCCATAAGCAGATCATATGACGATATCTGGGAGCATAAATCTTTGCTCTGTCCACAACAGTATATCCAGTGTCTTAGTTAGGGTTTTACTGCTGTGAACAGATATCATGACCAAGGCAAGTCTTATAAAAAACATTTAATTGGGGCTGGCTTACAGGTTCAGAGGTTCAGTCCATTATCATCAAGGTGGGAGCATGGCAGTATCCAGGTAG
19	Tmem132b	52.72	PCR failure	19			
20	Atp6v1h	52.56	PCR failure	20			
21	Rab2a	52.53	CTGACAGTGCTGTCCTGTGTATAC	CTGCTGGCTATCTTTGACAGTGC	363	222	CTGACAGTGCTGTCCTGTGTATACAAGCATAAATATTTAAAAGGCAATTTGGTGGCGTATTATGTCCAAATAACAGCAGAAGAATCCCAATTAAGGTCTATAACATTCAACCACAGGCTTTTCACTGGGTTTCTAGTACCAGATGTGAATTCATGCCTGTGGAGTGGGCCTCAAATTCAATACAAAAGCAGTTGTTTTTTTCCCAAAAATAACAGTCATGCAACTATGGTACTGGTGGGCACATATTGCCTGGAAGGTGGGTAGTCTGGCATGCAGAAGCCACAGCTGAGTCAGACTGTTGATGACAATTCTCCCCCAGAAGCCTACACAGACCCTTCTAGCACTGTCAAAGATAGCCAGCAG
22	Luc7l	52.44	TGCCTACATCAATCTGCAAGGGAG	GCAGTAAGGAAGTCGGGGAATG	311	136	TGCCTACATCAATCTGCAAGGGAGTTGCAGAAAAGCCTCATGTTCATCGAGCCGTGAGTCACAACCAATTTCTAAGCTGTTATAACAAAAAAGTGTTTGCTTTTTTCCCACAAGTAACTTTAAAAGTGTAGTTTAGAAAGAAAACATTTTCAGTAAAAAGACACGACATTAATCCTGGATGCTTGCCAATCCTGAAGTATATTCTCCCTGACTATTACACAGCACTGTGTCCTGTACACAGATAGCCTTAGAATTTGTCACATACCACTTTGCCTTTACTTTTATGTATCATTCCCCGACTTCCTTACTGC
23	Akr1b7	52.43	CTGGGCTGTACATCTGACATTCC	GCTAGCACAGCATTCCACCTATGA	281	135	CTGGGCTGTACATCTGACATTCCTCAGTGGAACAGGTGATAGGAGGGAAGGAGGACTCTTCTTCCCTGCCCTTCAGCTTCTCATCCCACTCTTTCACTGACAGTGTGTCTTCCCTTCTTCCAAGCACTCTGTCAACTTGTAGGCTAGAAAGCTGGGATGACTGAGCTCACAGGTGGTACCGGCCAAACCTGTCAGGACTGATCACAACTGTAGCTTATATCACTGAGATGACCACTGCCTACCATTGAGCACTTAGATCATAGGTGGAATGCTGTGCTAGC
24	Pvt1	52.4	GAAGCCAAAGGGAAGGGCAGG	CTTCCTGGATGCTGCCTTGTTC	310	175	GAAGCCAAAGGAAGGGCAGGAATATTTTTGTACCCTTGAATGCAATTAAATTCTAAAGCAGGTGTGAGGCTGAACTCTAGAACACAGCTTCCAACCCAGAGAAGGATACCTTGGACCTTCCTCTTTTTCCTCAGTCTGTAGAAGATACTGTCCTTACTTCAGGATGGTCTTAGTTAGGGTTTTACTGTTGTGAACAGATACCATGACCAATGTAAGTCTTATAAAGTACAACATTTAATTGGGGCTGACTTACAGTTTCCAAGATTCAGTCCATTATTGTCAAGGCAGGAACAAGGCAGCATCCAGGAAG

Supplementary Table 1. Details of the off-target analyses. The top off-targets are listed according to the ranking generated with TALENv.2 algorithm. The closest gene, the TALEN score, the forward and reverse primers sequence, and the amplicon size and sequence are indicated, as well at the predicted cleavage site.

ID	Closest Gene	WT MEFs untreated Total number of aligned reads	Reads with indels	Indel Frequency	nuclease treated Total number of aligned reads	Reads with indels	Indel Frequency	FA-A MEFs untreated Total number of aligned reads	Reads with indels	Indel Frequency	nuclease treated Total number of aligned reads	Reads with indels	Indel Frequency
1	Mbs85/Ppp1r12c	103938	109	0.10%	128806	47810	37.12%	107317	43	0.04%	97966	29534	30.15%
2	Vstm2b	120329	87	0.07%	110015	84	0.08%	81881	96	0.12%	105707	153	0.14%
3	Gcnt4	69690	74	0.11%	65566	44	0.07%	45999	37	0.08%	40663	26	0.06%
4	Opcml	91141	64	0.07%	55282	44	0.08%	117583	90	0.08%	95791	70	0.07%
5	Ush2a	100840	189	0.19%	78141	84	0.11%	90515	142	0.16%	113998	133	0.12%
6	Hs3st3b1	197005	134	0.07%	291378	205	0.07%	176089	120	0.07%	425033	338	0.08%
7	Gm15800	95634	54	0.06%	107987	54	0.05%	102713	69	0.07%	150677	83	0.06%
8	Pga5	115423	57	0.05%	91053	59	0.06%	38234	21	0.05%	43245	27	0.06%
9	4933402J15Rik	74900	70	0.09%	72764	62	0.09%	84815	67	0.08%	75574	71	0.09%
10	Odz4	195818	120	0.06%	201147	122	0.06%	200030	124	0.06%	185237	119	0.06%
11	Acbd6	92628	79	0.09%	83253	79	0.09%	86611	70	0.08%	76424	72	0.09%
12	Nkx6-1	95298	141	0.15%	87883	107	0.12%	102318	166	0.16%	88023	119	0.14%
13	Adam32	104306	93	0.09%	108741	396	0.36%	97994	108	0.11%	123054	403	0.33%
14	Cdh11	93757	69	0.07%	94248	55	0.06%	90752	51	0.06%	85379	70	0.08%
15	Gm5072	156935	30349	19.34%	145673	26758	18.37%	140998	25520	18.10%	142535	24233	17.00%
16	Cry1	66067	94	0.14%	71101	101	0.14%	67634	89	0.13%	72181	95	0.13%

17	Il20ra	71316	57	0.08%	77064	81	0.11%	76799	93	0.12%	63527	46	0.07%
18	Sec11c	73213	48	0.07%	84174	47	0.06%	75950	56	0.07%	61495	47	0.08%
19	Tmem132b	PCR failure											
20	Atp6v1h	PCR failure											
21	Rab2a	63093	112	0.18%	81971	200	0.24%	69384	118	0.17%	64857	126	0.19%
22	Luc7l	178913	413	0.23%	196906	199	0.10%	235926	283	0.12%	188185	221	0.12%
23	Akr1b7	111556	56	0.05%	95369	48	0.05%	121969	55	0.05%	104876	46	0.04%
24	Pvt1	112860	124	0.11%	113056	131	0.12%	116172	125	0.11%	111365	109	0.10%

Supplementary Table 2. Results of the next generation sequencing. The top off-targets are listed according to the ranking generated with TALENv.2 algorithm. The frequency of indels generated in each locus could be observed in WT MEFs and their respective counterparts, FA-A MEFs.

Purpose	Name	Sequence (from 5' to 3')	Tm (ºC)	Product size (pb)	Fluorochrome
qPCR *Sry*	Sry-F	TGTTCAGCCCTACAGCCACA	53.9	140	----------
	Sry-R	CCTCTCACCACGGGACCAC	54.8		----------
	Sry Probe	ACAATTGTCTAGAGAGAGCATGGAGGGCCA	64.7	----------	6-FAM
qPCR *β-Actin*	β-Actin-F	ACGGCCAGGTCATCACTATTG	53.9	131	----------
	β-Actin-R	ACTATGGCCTCAGGAGTTTTGTCA	55.9		----------
	β-Actin Probe	AACGAGCGGTTCCGATGCCCT	63.5	----------	Joe
PCR *T7E1* or *Cel1* assay	mAAVS1 CelIF	TCTGGATTCAGGATGCTTTT	54	405	----------
	mAAVS1 CelIR	TCACCTTGCTTCCACTTTCC	58		----------
5' PCR Integration junction	mAAVS1-5'F1	TTGTGGCCTCAGGACAGTGTAC	64	1167	----------
	mAAVS1-5'R1	AACGGACGTGAAGAATGTGCG	61		----------
	mAAVS1-5'F2	GGTTTCGTTCTCCTGCACTC	60	1439	----------
	mAAVS1-5'R2	GTCCGTCTGCGAGGGTACTA	63		----------
	mAAVS1-5'F3	TTCCCGTGACTTGTGCTGTA	64.4	1029	----------
	mAAVS1-5'R3	CCACGGGGTTGGGATTATTAT	65.2		----------
3' PCR Integration junction	mAAVS1-3'F1	ACAGATGGAAGGCCTCCTGG	63	1395	----------
	mAAVS1-3'R1	TCTTGGAACTTTCACTGCTAAAGC	62		----------
	mAAVS1-3'F2	GCAACCTCCCCTTCTACGAG	63	1337	----------
	mAAVS1-3'R2	GATGCCCCAAGGAGGGTTTA	60		----------
	mAAVS1-EGFP-3'F	GTGGTTTGTCCAAACTCATCAA	63.7	1035	----------
	mAAVS1-EGFP-3'R	TCCTTGTTTTCCTGGGACT	61.1		----------
PCR for sequencing 3' integration junction	mAAVS1-3'F2	GCAACCTCCCCTTCTACGAG	63	----------	----------
	mAAVS1-3'R2	GATGCCCCAAGGAGGGTTTA	60	----------	----------
	SequencingAAVS1-1_3'_F	TGGAGATGGGAAACAGAG	58.7	----------	----------
	SequencingAAVS1-2_3'_F	TGTCCCTAGAAGCTCTGGTG	62	----------	----------
	SequencingAAVS1-3_3'_F	CTGACTGCATCCCTCTCCTC	64	----------	----------
	SequencingAAVS1-4_3'_F	GCTTGGAAAGTGGAAGCAAG	63.8	----------	----------
	SequencingAAVS1-1_3'_R	TTGCATCTCCTTTCCCAATC	63.9	----------	----------

Supplementary Table 3. Primers and probes used in this study. Forward and reverse primers as well as probes, their sequence, their melting temperature (Tm) and the product size is indicated. In the case of probes, the fluorochrome to which each probe was conjugated is also indicated.

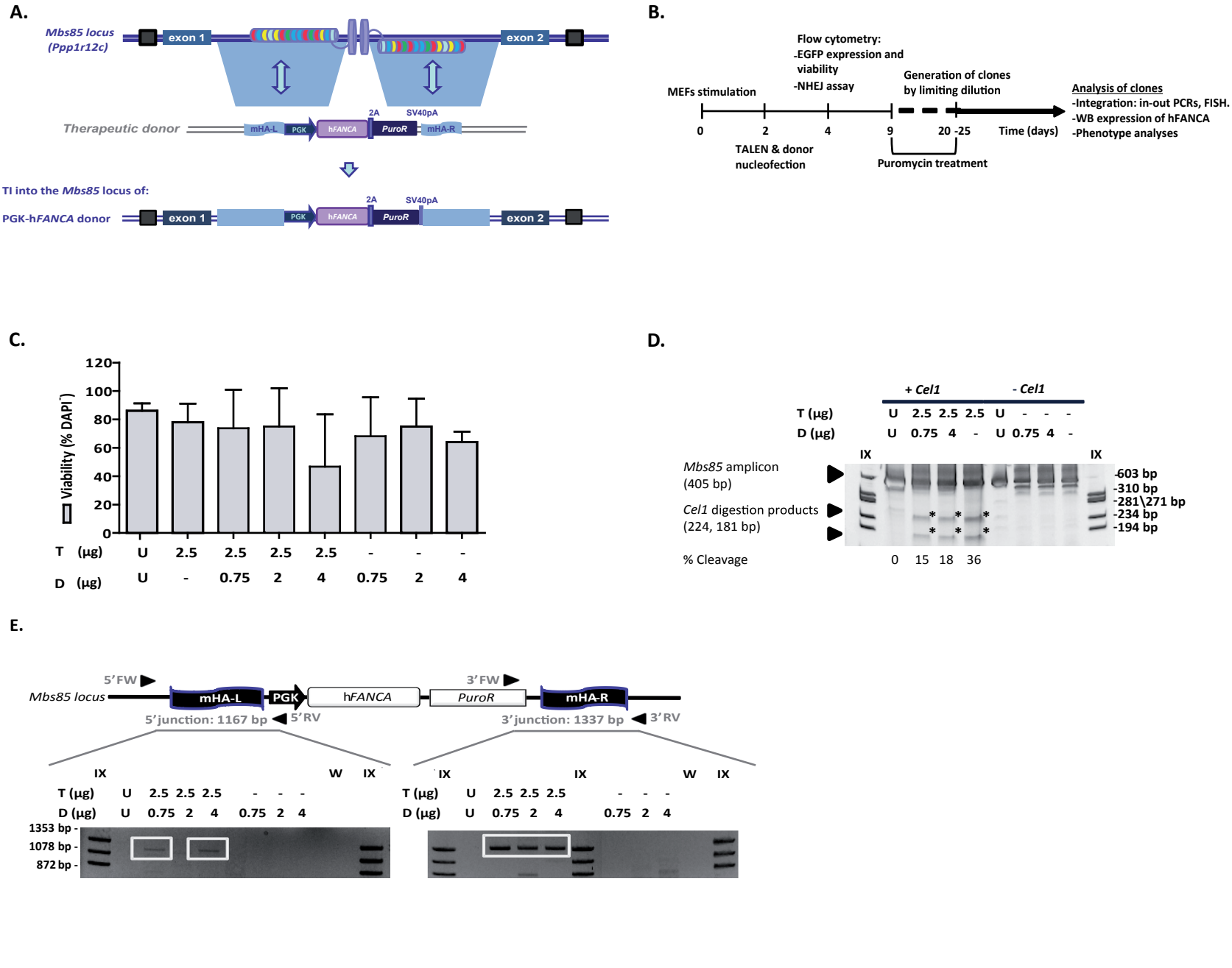
A.
Mbs85 locus (Ppp1r12c)
exon 1
exon 2
Therapeutic donor
mHA-L
PGK
hFANCA
2A
PuroR
SV40pA
mHA-R
TI into the Mbs85 locus of:
PGK-hFANCA donor
B.
Flow cytometry:
-EGFP expression and viability
-NHEJ assay
MEFs stimulation
Generation of clones by limiting dilution
Analysis of clones
-Integration: in-out PCRs, FISH.
-WB expression of hFANCA
-Phenotype analyses
0
2
4
9
20 -25
Time (days)
TALEN & donor nucleofection
Puromycin treatment
C.
Viability (% DAPI-)
120
100
80
60
40
20
0
T (µg) U 2.5 2.5 2.5 2.5 - - -
D (µg) U - 0.75 2 4 0.75 2 4
D.
+ Cel1
- Cel1
T (µg) U 2.5 2.5 2.5 U - - -
D (µg) U 0.75 4 - U 0.75 4 -
IX
IX
Mbs85 amplicon (405 bp)
Cel1 digestion products (224, 181 bp)
603 bp
310 bp
281\271 bp
234 bp
194 bp
% Cleavage
0 15 18 36
E.
5'FW
3'FW
Mbs85 locus
mHA-L
PGK
hFANCA
PuroR
mHA-R
5'junction: 1167 bp
5'RV
3'junction: 1337 bp
3'RV
IX
W
IX
T (µg) U 2.5 2.5 2.5 - - -
D (µg) U 0.75 2 4 0.75 2 4
1353 bp
1078 bp
872 bp

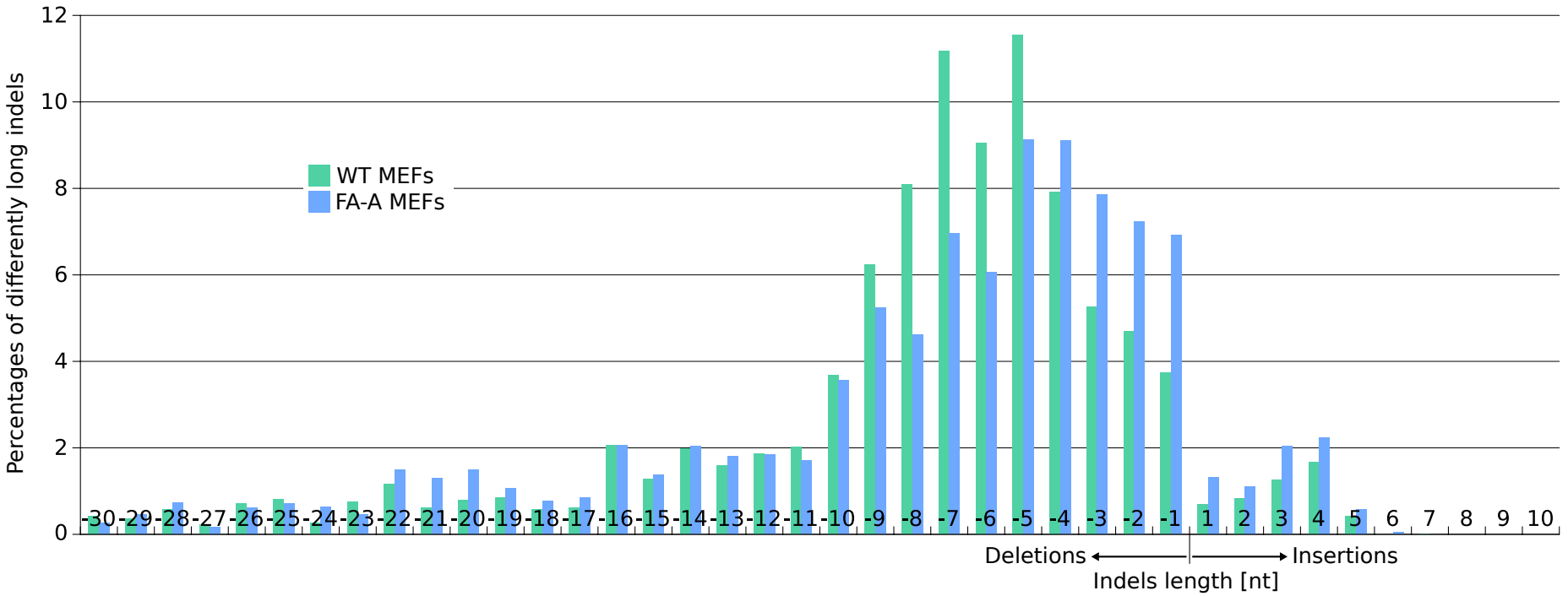
Percentages of differently long indels
12
10
8
6
4
2
0
WT MEFs
FA-A MEFs
-30 -29 -28 -27 -26 -25 -24 -23 -22 -21 -20 -19 -18 -17 -16 -15 -14 -13 -12 -11 -10 -9 -8 -7 -6 -5 -4 -3 -2 -1 1 2 3 4 5 6 7 8 9 10
Deletions
Insertions
Indels length [nt]

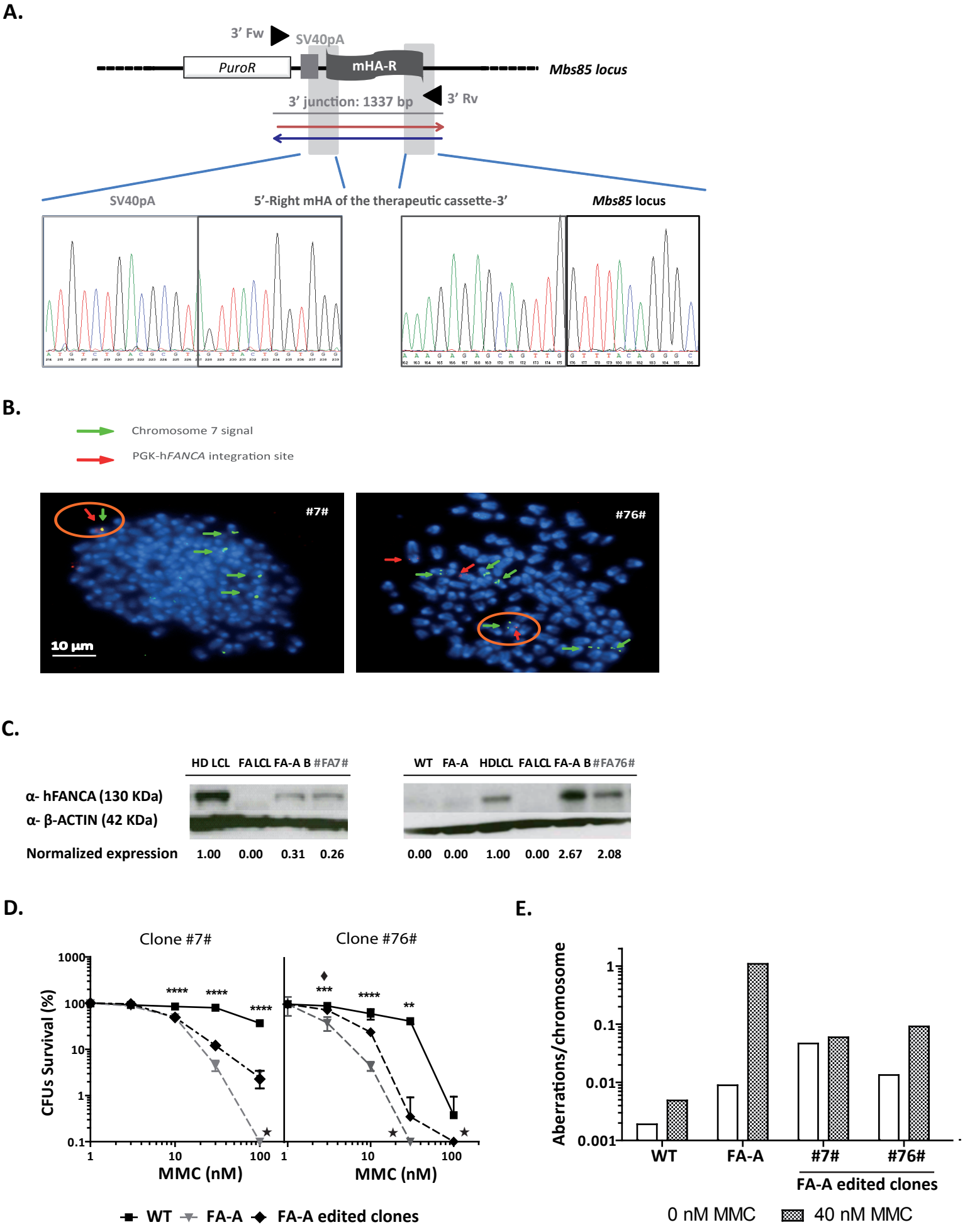
A.
3' Fw
SV40pA
PuroR
mHA-R
Mbs85 locus
3' junction: 1337 bp
3' Rv
SV40pA
5'-Right mHA of the therapeutic cassette-3'
Mbs85 locus
B.
Chromosome 7 signal
PGK-hFANCA integration site
#7#
#76#
10 µm
C.
HD LCL
FA LCL
FA-A B
#FA7#
WT
FA-A
HDLCL
FA LCL
FA-A B
#FA76#
α- hFANCA (130 KDa)
α- β-ACTIN (42 KDa)
Normalized expression
1.00 0.00 0.31 0.26
0.00 0.00 1.00 0.00 2.67 2.08
D.
Clone #7#
Clone #76#
CFUs Survival (%)
MMC (nM)
MMC (nM)
WT
FA-A
FA-A edited clones
E.
Aberrations/chromosome
WT
FA-A
#7#
#76#
FA-A edited clones
0 nM MMC
40 nM MMC

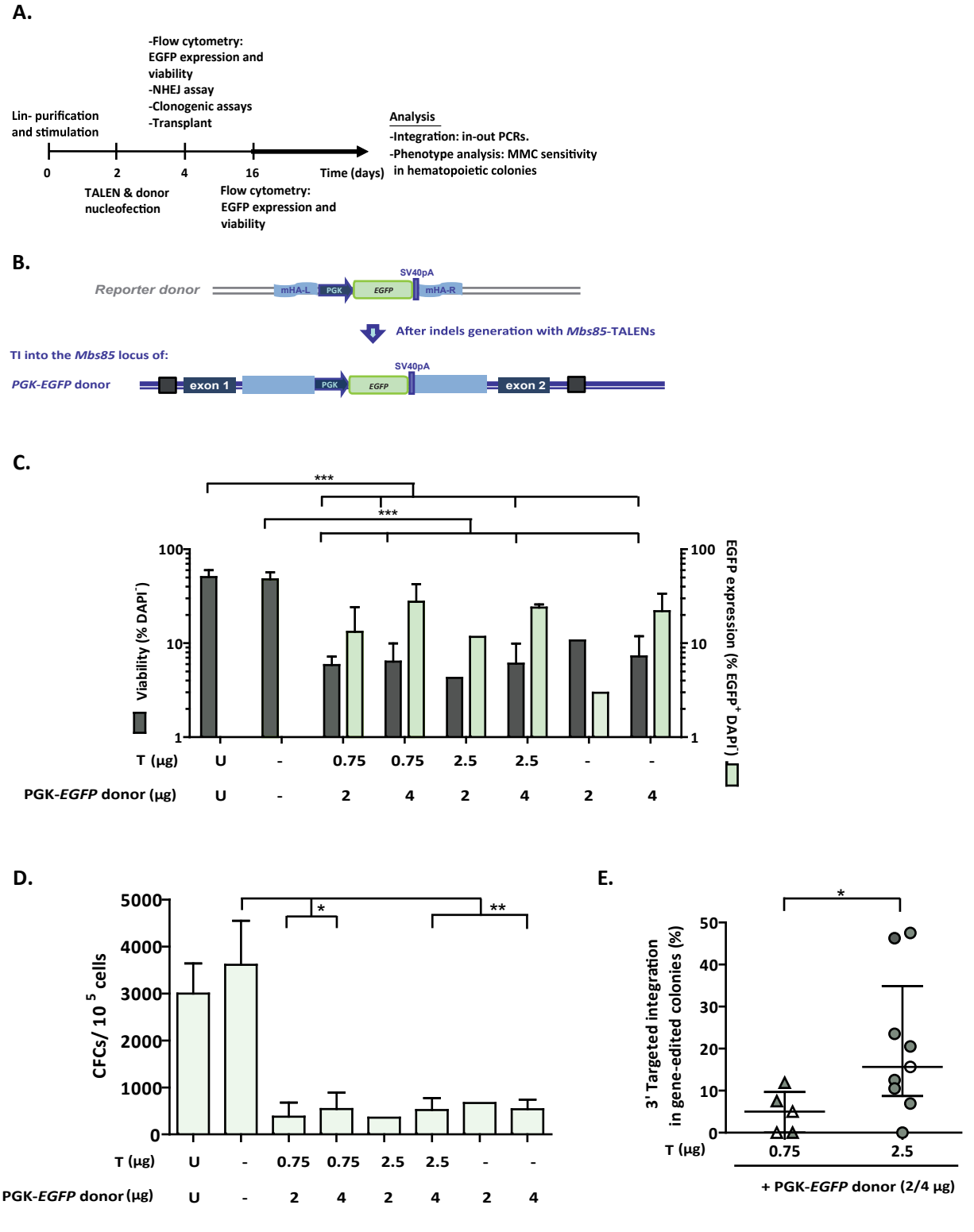
A.
-Flow cytometry:
EGFP expression and
viability
-NHEJ assay
-Clonogenic assays
-Transplant
Lin- purification
and stimulation
Analysis
-Integration: in-out PCRs.
-Phenotype analysis: MMC sensitivity
in hematopoietic colonies
0
2
4
16
Time (days)
TALEN & donor
nucleofection
Flow cytometry:
EGFP expression and
viability
B.
Reporter donor
SV40pA
mHA-L
PGK
EGFP
mHA-R
After indels generation with Mbs85-TALENs
TI into the Mbs85 locus of:
PGK-EGFP donor
SV40pA
exon 1
PGK
EGFP
exon 2
C.
***
***
***
100
10
1
Viability (% DAPI-)
100
10
1
EGFP expression (% EGFP+ DAPI-)
T (µg)
U
-
0.75
0.75
2.5
2.5
-
-
PGK-EGFP donor (µg)
U
-
2
4
2
4
2
4
D.
5000
4000
3000
2000
1000
0
CFCs/ 10 5 cells
*
**
T (µg)
U
-
0.75
0.75
2.5
2.5
-
-
PGK-EGFP donor (µg)
U
-
2
4
2
4
2
4
E.
*
50
40
30
20
10
0
3' Targeted integration
in gene-edited colonies (%)
T (µg)
0.75
2.5
+ PGK-EGFP donor (2/4 µg)

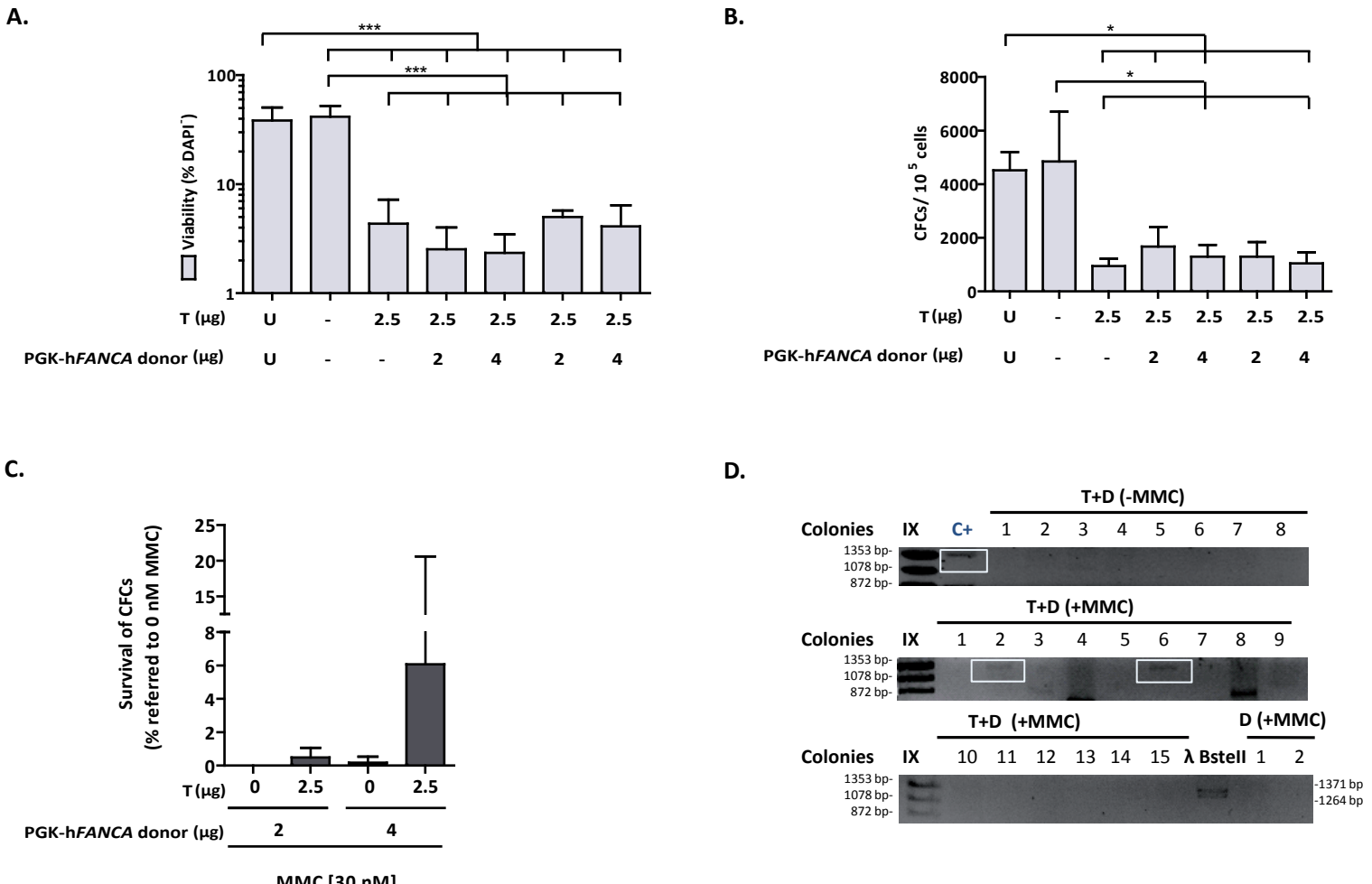
A.
***
***
100
10
1
Viability (% DAPI-)
T (µg) U - 2.5 2.5 2.5 2.5 2.5
PGK-hFANCA donor (µg) U - - 2 4 2 4
B.
*
*
8000
6000
4000
2000
0
CFCs/ 10 5 cells
T (µg) U - 2.5 2.5 2.5 2.5 2.5
PGK-hFANCA donor (µg) U - - 2 4 2 4
C.
Survival of CFCs
(% referred to 0 nM MMC)
25
20
15
8
6
4
2
0
T (µg) 0 2.5 0 2.5
PGK-hFANCA donor (µg) 2 4
MMC [30 nM]
D.
T+D (-MMC)
Colonies IX C+ 1 2 3 4 5 6 7 8
1353 bp-
1078 bp-
872 bp-
T+D (+MMC)
Colonies IX 1 2 3 4 5 6 7 8 9
1353 bp-
1078 bp-
872 bp-
T+D (+MMC)
D (+MMC)
Colonies IX 10 11 12 13 14 15 λ BsteII 1 2
1353 bp-
1078 bp-
872 bp-
-1371 bp
-1264 bp